Energy, Mines and Resources Canada
Earth Physics Branch
1 Observatory Crescent
Ottawa Canada
K1A 0Y3

Énergie, Mines et Ressources Canada
Direction de la physique du globe
1 Place de l'Observatoire
Ottawa Canada
K1A 0Y3

Geodynamics Service of Canada

Service de la géodynamique du Canada

ESTABLISHMENT AND ANALYSIS OF PRECISE GEODETIC NETWORKS: VANCOUVER ISLAND 1982-1984

W.F. Slawson and M. Lisowski
Department of Geophysics and Astronomy
University of British Columbia

Earth Physics Branch Open File Number 85-4
Dossier public de la Direction de la Physique du Globe No. 85-4
Ottawa, Canada

pp. 81
Price / Prix : $16.31

Preface

This open file consists of the final report to the Earth Physics Branch for the project entitled: "Establishment and Analysis of Precise Geodetic Networks: Vancouver Island". The work was carried out under the E.M.R. Research Agreements Program over a period of two years commencing in 1982. Field measurements were made in the Gold River region on the west coast of central Vancouver Island in the summers of 1982 and 1983, and involved personnel from the Geodetic Survey of Canada, the Earth Physics Branch, and the University of British Columbia. This project also comprises the basis of an M.Sc. thesis for the Department of Geophysics and Astronomy, U.B.C., by M. Lisowski.

More than half of this report concentrates on instrumentation and survey techniques required to carry out horizontal control surveys with a precision of several parts in 10^7. The measurement of temperature and humidity along lines of sight, being a primary requirement for such precision, is dealt with in detail. The latter part of the report compares the original 1947 triangulation data with the trilateration data of 1982 and 1983. The method of Frank (1967) is used to estimate net shear strain for the Gold River region over a 35 year period.

H. Dragert
Pacific Geoscience Centre
September, 1984

Résumé

Le présent dossier public renferme le rapport final présenté à la Direction de la physique du globe sur le projet intitulé: "Establishment and Analysis of Precise Geodetic Networks: Vancouver Island". Les travaux ont été menés dans le cadre du Programme des conventions de recherche d'EMR sur une période de deux ans, à partir de 1982. Le personnel provenant de la Division des levés géodésiques du Canada, de la Direction de la physique du globe et de l'Université de la Colombie-Britannique a fait des mesures sur le terrain dans la région de Gold River sur la côte ouest de la partie centrale de l'île de Vancouver durant les étés 1982 et 1983. Le projet consitue aussi le fondement d'une thèse de maîtrise ès sciences par M. Lisowski du département des sciences de la Terre et de l'astronomie, de l'Université de la Colombie-Britannique.

Plus de la moitié du rapport décrit les instruments et les techniques de relevés qui sont nécessaires pour établir le canevas planimétrique avec une précision de plusieurs parties par 10^7. Il traite en détail de la mesure de la température et de l'humidité le long de la ligne de visée, exigence primordiale pour obtenir une telle précision. La seconde partie du rapport compare les données de la triangulation de 1947 avec celles de la trilatération de 1982 et de 1983. La méthode de Frank (1967) est utilisée pour estimer la déformation nette au cisaillement dans la région de Gold River sur une période de 35 ans.

H. Dragert
Centre géoscientifique du Pacifique
Septembre 1984

Final Report
EMR Research Agreement

Establishment and Analysis of Precise Geodetic Networks: Vancouver Island 1982-1984

W.F. Slawson and M. Lisowski

March 31, 1984

The University of British Columbia

Introduction

Repeated geodetic surveys provide a measure of the surface deformation in the area covered by the measurements. In seismically active areas the rate of deformation along with the repeat time of large earthquakes allow an estimate of the seismic hazard (Thatcher, 1981). This summary details measurements of a precise trilateration network, the Gold River network, located in the central part of Vancouver Island (see Figure 1.1). Central Vancouver Island has experienced several large (M=6.0) and two major (M=7.0) earthquakes within the last 67 years. Future surveys of the Gold River network may aid in unravelling the tectonic pattern responsible for these earthquakes by defining the rate and pattern of deformation.

The measurements were made by the Surveys and Mapping Branch of the Department of Energy, Mines, and Resources, with aid from H. Dragert of the Earth Physics Branch and W.F. Slawson and M. Lisowski of the University of British Columbia. The results from instrument calibration tests and intercomparisons are reported along with an estimate of the error in a distance measurement and the corresponding strain resolution. Recommendations for further instrument tests and modifications in procedures are offered. Finally, the 1982 survey is compared with a 1947 triangulation survey to deduce shear strain accumulation in the interval between the surveys.

Table of Contents

1. 1982 GOLD RIVER SURVEY

In 1982 a high precision trilateration network was established near the town of Gold River in central Vancouver Island. The network includes a portion of a triangulation network surveyed during 1946 and 1947. The primary goals of the project were to establish a network capable of resolving strain accumulation at the 0.3ppm level and to tie this network into the existing triangulation network to determine strain accumulation between 1947 and 1982.

This section serves to document the measurements, the equipment, and the methods used in the 1982 survey. Four types of measurements were made, distances corrected for refractivity with aircraft flown meteorological profiles, distances corrected with end point meteorological readings, horizontal angles, and simultaneous reciprocal vertical angles. All measurements were made by the Surveys and Mapping Branch of the Dept. of Energy, Mines, and Resources which will be referred to as the Canadian Geodetic Survey (CGS).

The primary distance measurements are those corrected for refractivity with aircraft flown profiles. The 23 lengths measured are shown in Figure 1.1, and listed in Table 1.1.

Ties to the 1947 stations were made with distance measurements corrected from end-point meteorological readings, and horizontal angles. These distances and angles are shown in Figure 1.2 and listed in Tables 1.1 and 1.2.

Table 1.1. 1982 Distances

Complete meteorology

STA 1	STA 2	M-M DIST* (m)	CLARKE-ARC** (m)
Albermarle G	Ana	23499.927	23495.845
	Baldy G	30811.412	30800.206
	New	32393.728	32385.591
	Pierce	24998.291	24991.146
	Pretty G	17239.587	17236.127
Ana	Baldy G	29940.256	29929.987
	New	17347.225	17341.366
	Pierce	36034.882	36026.707
Baldy G	Gold	16210.979	16206.246
	New	18531.153	18525.770
	Pierce	15771.634	15766.626
	Pretty G	28429.760	28420.447
	Sentinel	25197.822	25190.885
	Twaddle	28994.216	28986.213
Gold	New	23948.638	23940.614
	Pierce	30199.231	30190.044
	Sentinel	9173.344	9170.847
	Twaddle	21880.387	21874.411
New	Sentinel	29034.043	29025.073
	Pierce	31302.719	31295.846
	Twaddle	18533.580	18525.792
Pierce	Pretty G	14700.131	14695.518
Sentinel	Twaddle	20231.954	20227.427

End-point meteorology

Pretty G	Pretty	3.316	TAPED
Albermarle G	Albermarle	1.045	TAPED
Ana	Walker	4938.152	4937.163
Albermarle G	Pretty	17237.488	17234.002
Twaddle	Wanch	5097.872	5094.194
Baldy G	Baldy	28.448	27.916
New	Conuma***	4343.561	4341.999
Gold	Conuma***	22784.861	22777.772
Pierce	Conuma***	26977.224	26971.031
Pierce	Rufus***	17352.451	17346.938
Pretty G	Rufus***	12000.566	11998.290
Baldy G	Rufus***	24405.312	24395.561

* M-M distance is mounument to monument distance.
** Clarke-arc distance is the distance between the projections of the monuments onto the 1866 Clarke spheroid.
*** Measurements made in July, 1983.

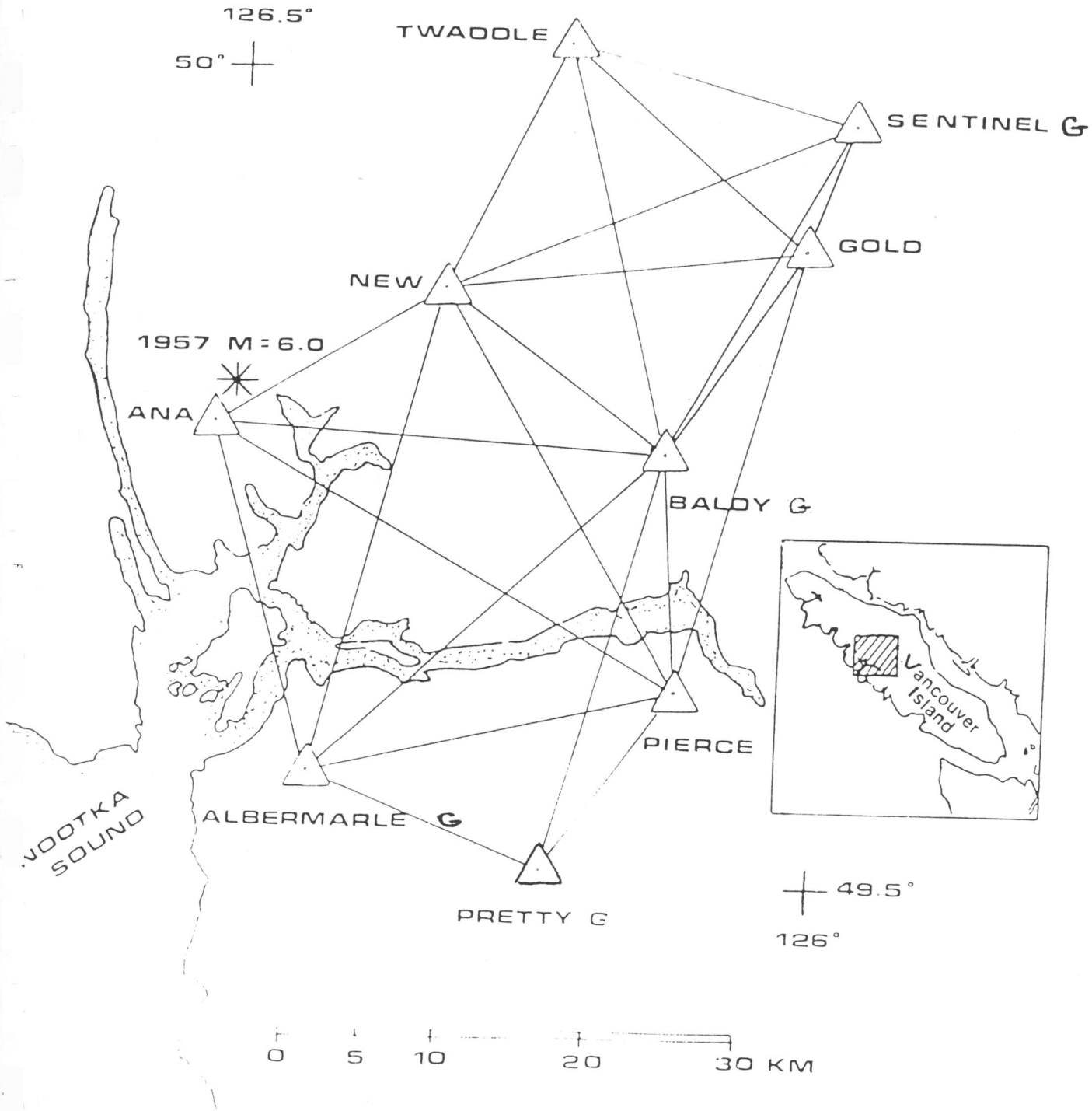

Figure 1.1. Map showing 1982 trilateration network. Inset shows the location of the network and the * indicates the epicenter of the 1957 M=6.0 earthquake.

Table 1.2. Horizontal angles

Inst Sta	Initial Sta	Target Sta	Angle ° ' "
Baldy	Gold	Baldy G	240 49 07.67
Baldy G	Gold	Baldy	60 43 45.24
Twaddle	Gold	Wanch	16 55 58.52
Pretty G	Pierce	Pretty	207 11 08.25
Albermarle G	Pretty	Albermarle	99 00 22.75
Ana	Walker	Pierce	69 10 21.91

The simultaneous reciprocal vertical angles provide elevation control. The vertical angles measured are shown in Figure 1.3 and derived elevations (provided by the CGS) are listed in Table 1.3.

To allow comparison with horizontal angles measured in 1947 the distances and angles are used to find the most probable positions for the stations. The slope distances are reduced to the 1866 Clarke Spheroid (Clarke-arc distances) using the station elevations and azimuth of the line (Bomford, 1971). The elevations are referenced to the geoid with no correction made for the difference between the geoid and the Clarke spheroid. The Clarke-arc distances and measured horizontal angles are then used to find the most probable station positions with a variation of coordinates adjustment (Anderson, 1969). The position of Pierce and the azimuth to Gold were arbitrarly fixed to remove translational and rotational ambiguities. The derived latitudes and longitudes are not fixed to an external framework and, therefore, should not be used for horizontal control. The positions determined from the local adjustment are listed along with the elevations in Table 1.3.

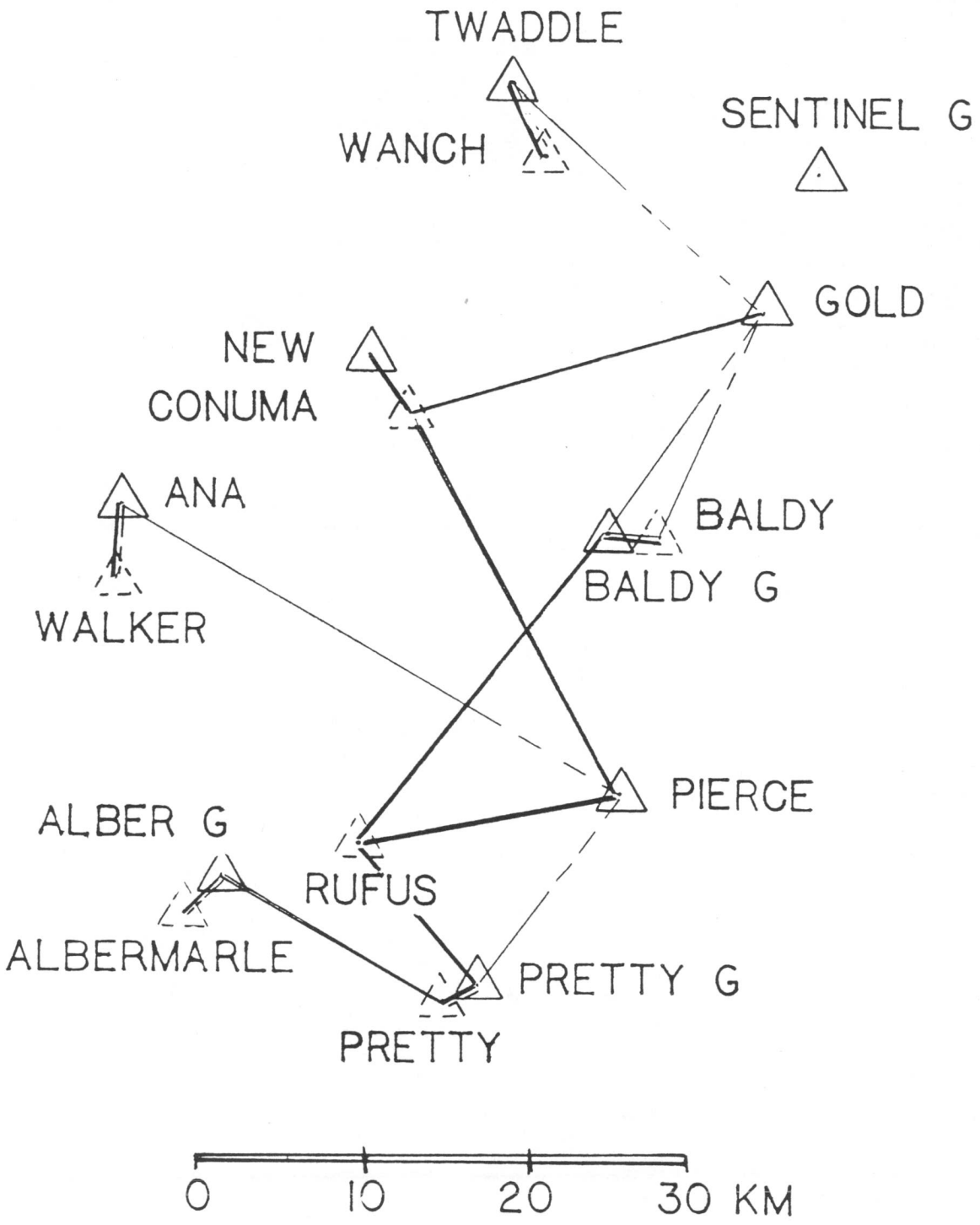

Figure 1.2. Sketch of the horizontal ties between 1947 and 1982 survey monuments. 1982 monuments are indicated by sold triangles and 1947 monuments by dashed triangles. Gold, Pierce, and New are common to both surveys. Distances measurement are shown as solid heavy lines and horizontal angles by the thin lines with the dashed end indicating the station sighted. Scale will be distorted for nearby stations.

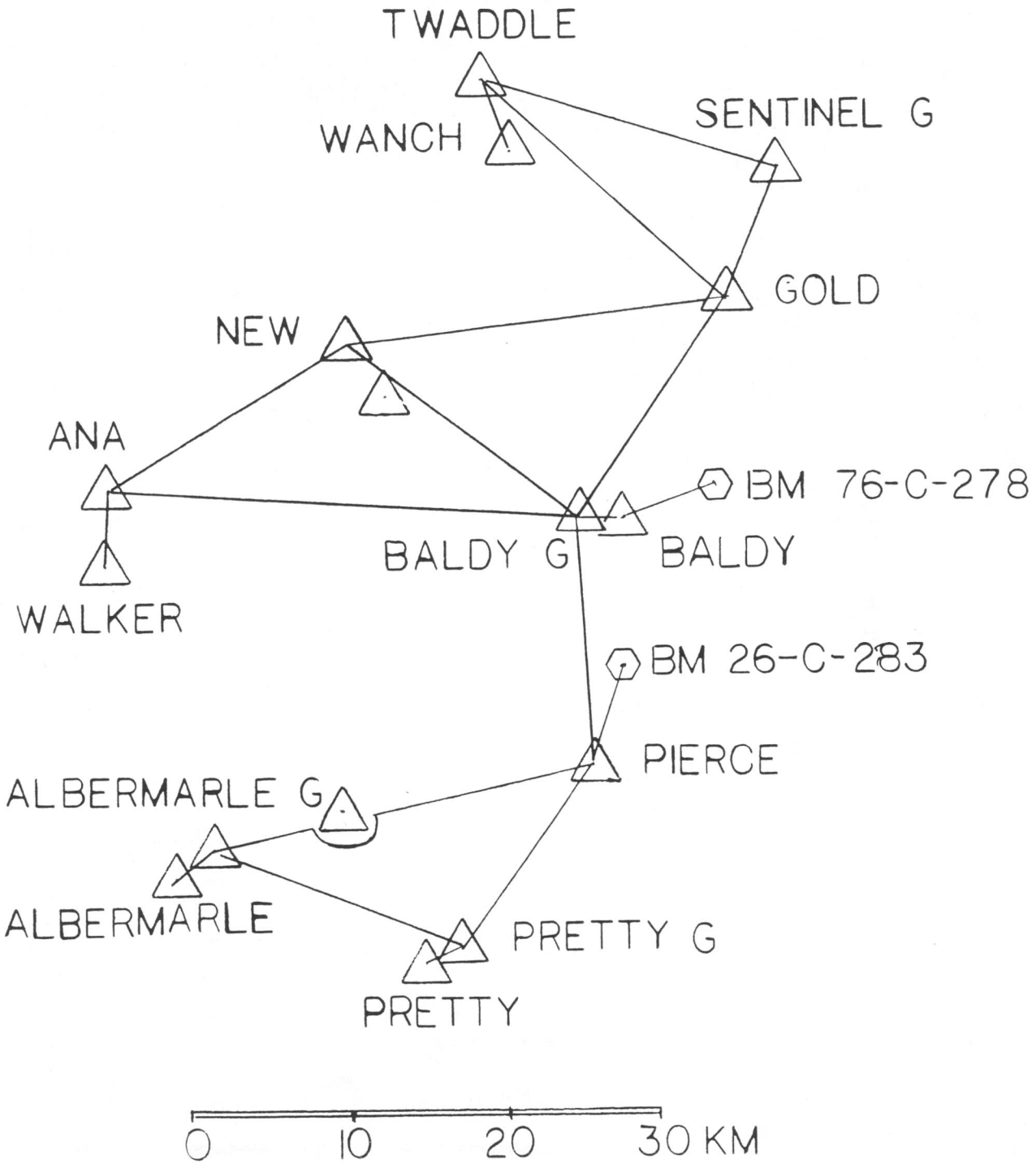

Figure 1.3. Map showing simultaneous reciprocal vertical angles observed during the 1982 survey. Vertical control benchmarks are indicated with hexagons. Both Albermarle and Pretty are tied by non-reciprocal vertical angles.

Table 1.3 Elevations, Latitudes, and Longitudes

Station	Elev (m)	Latitude ° ' "	Longitude ° ' "
Albermarle	1060.62	40 35 05.9885	126 27 43.7807
Albermarle G	1060.15	49 35 06.0162	126 27 43.7509
Ana	1120.25	49 47 21.1530	126 32 43.9345
Baldy	1609.87	49 45 38.5043	126 07 55.1204
Baldy G	1604.44	49 45 38.5996	126 07 56.5074
Gold	1731.60	49 52 46.3094	126 00 07.1901
New	1410.51	49 51 50.7839	126 20 02.9955
Pierce	1402.56	49 37 09.0340	126 07 13.6490
Pretty	1183.56	49 30 59.6042	126 14 54.5662
Pretty G	1183.11	49 30 59.6160	126 14 54.5830
Sentinel G	1737.73	49 57 23.4540	125 57 22.5948
Twaddle	1754.68	50 00 52.4932	126 13 24.7185
Walker	1152.90	49 44 44.1149	126 33 29.6111
Wanch	1600.83	49 58 29.3728	126 11 17.7400
Rufus	1134.2*	49 35 56.9338	126 21 29.2507
Conuma	1481.3*	49 49 43.2470	126 18 31.7172

* Elevations from B.C. Ministry of Surveys

1.1 GENERAL THEORY OF EDM MEASUREMENTS

This subsection explains some of the rudimentary concepts of an electronic distance meter (EDM) measurement. The scale correction to a measured length due to atmospheric conditions is discussed and the form of the equation for the group refractive index is expressed.

The Rangemaster III, used for all EDM measurements in this project, transmits an intensity modulated laser beam that is returned to the instrument by retro-reflector prisms. The returned signal is focused on a photo-detecting diode by the receiving telescope. A phase delay in the modulated beam is introduced by the transit time in the two-way path between the instrument and retro-reflector. Comparison of the outgoing and incoming modulations gives the phase shift. This shift varies

with the distance of the two-way travel path and the modulation length. Thus, the distance is resolved into an unknown number of whole modulation lengths plus a known fractional modulation length.

$$L = 1/2(M + \theta/2\pi)\lambda m \qquad (1.1)$$

where L is the length, M is an unknown number of whole modulation lengths $\theta/2\pi$ is the phase shift, and λm is the modulation length.

The two-way travel path makes the effective modulation length equal to 1/2 wavelength, since moving the reflector 1 m toward the instrument will shorten the path length by 2 m.

The modulation length is equal to the ratio of the group velocity, Vg, with which the modulation is transmitted to the modulation frequency, fm.

$$\lambda m = Vg/fm$$

The group velocity of the modulated light varies with the average value of the group refractive index of the air it passes through, nGA.

$$Vg = c/nGA$$

where c is the velocity of light in a vacuum.

Accurate formulae for the group refractive index of air as a function of composition, pressure, temperature, water vapor pressure, and carrier wavelenth are known (Owens, 1967).

Distance measurements are actually made using a nominal modulation wavelengh λn and later corrected for the difference between the nominal refractive index, nGN, and the measured value, nGA. The modulation wavelength is expressed as

$$\lambda m = \lambda n(nGN/nGA) \qquad (1.2)$$

where λn the nominal modulation length is found by

$$\lambda n = c/(fm \cdot nGN)$$

Fixing the nominal wavelength to a whole number distance, λn=20 m, specifying a nominal refractive index (nGN=1.000310) and using c=299,792.5 km/s yields a nominal modulation frequency of 14,984,979.7 Hz. Substituting for λm in (1.1) from (1.2) gives

$$L = 1/2(M + \theta/2\pi) \cdot \lambda n(nGN/nGA)$$

Resolving the length ambiguity by using several different and well-chosen nominal modulation lengths we can write

$$L = Lm \cdot (nGN/nGA)$$

where Lm is the measured length

The ratio of the nominal refractive index to the measured refractive index is the refractive index scale correction to a distance measurement. This scale correction is generally much less than the shortest modulation length and not important in the coarse distance calculation. An additional scale correction may be necessary if the modulation frequency drifts from the nominal value. This correction is merely the ratio of the nominal modulation frequency to the actual modulation frequency.

Only the actual refractive index remains to be determined. The Owens' formula for the group refractive index of air is of the form (Owens, 1967)

$$nGA = 1 + RsDs + RwDw$$

where Rs and Rw are constants dependent on the carrier wavelengh in a vacuum. For the Rangemaster III the carrier wavelength is 0.6328 μm and Rs = 8087.6 and Rw = 6909.7.
Ds is the density factor of dry air containing 0.03% CO_2 of temperature T (K) and with partial pressure Ps (mb)

$$Ds = (Ps/T)[1 + Ps(57.90 \cdot 10^{-8} - (9.3250 \cdot 10^{-4}/T) + 0.25844/T^2)]$$

and Dw is the density factor of moist air at temperature T (K) with partial pressure Pw (mb)

$$Dw = Pw/T\{1+Pw[1+(3.7\cdot10^{-4})Pw]$$
$$\cdot[-2.37321\cdot10^{-3} + 2.23366/T - 710.792/T^2 + 7.75141\cdot10^4/T^3]\}$$

Ignoring factors such as the curvature of the light path and additive constants, the accuracy of a distance measurement depends on the stablity of the modulation frequency and the accuracy of the average refractive index.

The following scale corrections give an idea of the change in a distance measurement caused by a variation in the average pressure, temperature, and humidity.

About a 1ppm increase in length is produced by any of the following:

a 1°C increase in the average temperature

a 0.34 kPa decrease in the average pressure (equivalent to a 3.4 mb, 2.5 mm, or 0.1 in decrease).

at 20°C a 100% increase in the relative humidity or

at 35°C a 50% increase in the relative humidity.

With oven controlled quartz crystal oscillators stable to about 0.1ppm, the principal limitation to the accuracy of a distance measurement is the uncertainty of the average temperature, pressure, and humidity of the air along the path.

1.2 EQUIPMENT AND PROCEDURES

Of the four types of measurements made during the 1982 survey of the Gold River network, only the distance measurements corrected with aircraft flown temperature and humidity profiles use non-standard surveying techniques. The following discussion concerning equipment and procedures is limited to these distance measurements. The discussion is divided into three areas; 1) the distance meter and reflectors, 2) aircraft mounted probes, and 3) pressure sensors.

1.2.1 DISTANCE METER

A Keuffel and Esser Rangemaster III was used to make all distance measurements. It is a long range (>40 km maximum) electro-optical distance meter using a 5 mW helium-neon laser (carrier wavelength of 0.6328 μm) that is amplitude modulated at a nomimal frequency of 14,984,979.7 Hz. The manufacturer specifies an accuracy of 5 mm±1ppm. A discussion of the internal workings and the related intrumental errors may be found in Berg et al (1981). Summarizing their discussion and that of Greene (1977), the main sources of instrumental error are modulation frequency stability, pointing error, zero error, non-linearity in the phase detector, receiver noise, and error related to the amplitude of the return signal.

The short term stability of the modulation frequency was tested by the Geodetic Survey over a temperature range of 0° to 23°C. After a 20 minute warm-up, drift in the modulation

frequency over a 7 hr period of continuous operation was less than 0.05ppm. A plot of the frequency drift over time from these tests is shown in Figure 1.4. Possible long term drift of the modulation frequency was checked during the Gold River survey by daily measurements with a portable frequency standard. Over the period of the survey the modulation frequency remained within 0.05ppm of the nominal value. The measured drift would produce less than a 1.5mm change in the longest (35km) line. Because the measured frequency drift is within possible error in the time base of the portable frequency counter, the reduced distances (Table 1.1) do not include a scale correction for drift in the modulation frequency.

Pointing error may occur when the return beam does not illuminate the entire area of the receiver optics. Short measurements (<300m) to retro-reflector are particularly sensitive to pointing error. Pointing error may be asessed by comparing the distances measured with the return beam illuminating different parts of the receiving telescope. If the span is greater than 10mm it indicates misaligment of the optics. During long measurements, the random scattering of the beam tends to average out the pointing error.

Constant error in a measured length results from the combination of errors in the instrument and reflector correction constants and the linearity of the phase detector. It is assumed that the instrument constant is independent of the length. Short term fluctuations in the electronic center

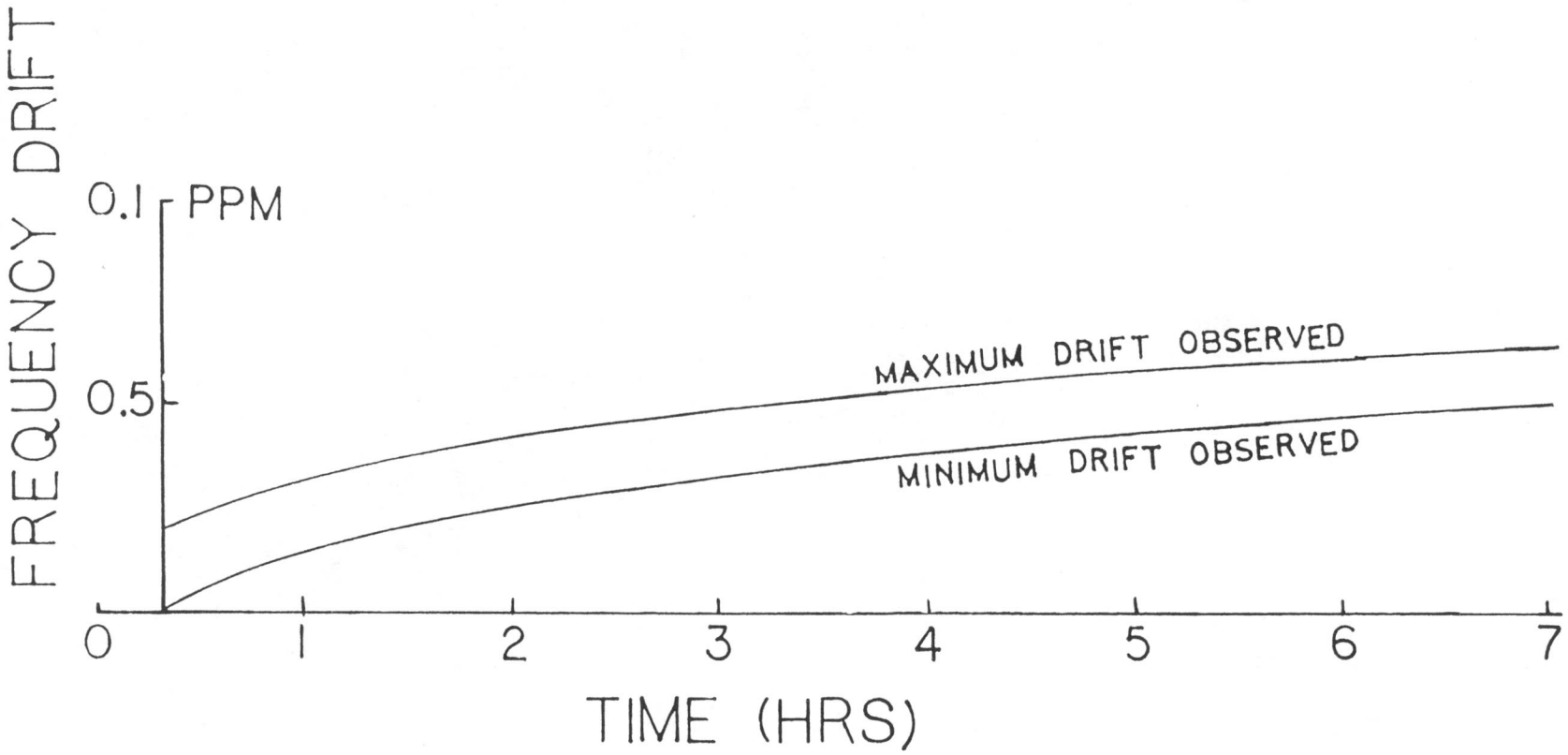

Figure 1.4. Plot of ppm drift in the modulation frequency as a function of operating time in hours. The envelope encloses the range of readings taken over 7 days at ambient temperatures from 0° to 23°C.

of the instrument are automatically corrected by the Rangemaster III during ranging by alternating range measurements with measurements of an internal fiber optics path. The small unknown phase shifts introduced by the electronic components affect each measured length by the same amount. The displayed distance is the difference between the instrument-reflector distance and the internal path distance. The instrument constant corrects for this internal path length and any constant offset between the electro-optical and mechanical center of the instrument. The reflector constant corrects for the offset introduced by the reflector and its mount. The zero error results from error in the instrument constant and reflector constant. Non-linearity in the phase detector results in cyclic error which varies over one effective wavelength (10 m). It is due to electrical and/or optical leakage between the modulator and the receiver electronics or optics. This error tends to be sinusoidal over the effective wavelength with a maximum amplitude of ±5mm for the Rangemaster III. Tests made to check the instrument constant are discussed at the end of this section.

On long range measurements where the return signal is relatively weak, noise in the photo-detector and receiver contribute to measurement error. Noise tests (Berg et al., 1981, p 22) indicate a 2 mm contribution to the standard deviation of a length.

The Rangemaster III only acquires distance measurements when the return signal strength is within a specified range.

The return signal strength is adjusted by the operator by means of a grey wedge filter. On long lines, or under turbulent conditions the return signal strength varies considerably requiring frequent adjustment. The zero-crossing detector is sensitive to the return signal level, thus measurements made at the upper and lower limits of acceptable signal may differ. No tests were made to determine the magnitude of this error, but care was taken to keep the signal balanced during all measurements.

1.2.1.1 Instrument constant

Measurements of the Victoria baseline were made before and after the Gold River survey to check the instrument constant. The 1.7 km Victoria baseline consists of a set of 6 piers with forced centering mounts. Reference baseline distances are derived from an adjustment of Mekometer surveys made in 1975, 1977, and 1978. The Mekometer is a high precision short-range distance meter with a precision of ±1ppm (Rinner, 1974).

Measurement of a distance of known length determines the total correction resulting from the sum of the instrument constant, reflector constant, and the non-linearity. Generally, short baselines are used to reduce refractivity related scale error, but then pointing error may contaminate short distance measurements.

The distance between 3 piers separated by 230, 953, and 1582 m were measured with the Rangemaster III in 1982. End point meteorological readings were used to correct for

refractivity. Rangings at each distance were made to two different reflectors in a single mount and to two different sets of two reflectors in the 16-reflector mount that was used for all the Gold River measurements. The square 16-reflector mount requires uncovering at least two of the central reflectors to assure symmetry about the vertical rotation axis. The reduced pier to pier distances and the derived instrument constant assuming a relector constant of -0.030 m (specified by the CGS) are listed in Table 1.4. Each listed distance represents the average of about 20 readings. There does not appear to be any systematic difference between the single and 16-reflector mounts, or between the 6 July and 24 July 1982 surveys. The standard deviation of the instrument constant from the 7 measurements at each distance varies between 2 and 5mm. The mean instrument constant from these test is 0.138±0.004 m. The instrument constant used in the reduction of the distances measured in the Gold River survey is 0.140 m. This value was obtained by the CGS from baseline measurements in Ottawa taken before and after the Gold River survey.

The relative contribution of pointing error, meteorological error, non-linearity, and baseline error are not known. Pointing error is probably significant in only the 230 m distance, as the beam diverges enough to illuminate the entire receiving telescope at the 953 and 1582 m distances.

Table 1.4. Victoria baseline RM III #8016

Date	Inst Sta	Refl Sta	M-M dist (m)	Inst. constant	Refl. ID	Mount style
6 July 82	Pier 2	Pier 5	1582.384	0.133	#35	single
			1582.393	0.129	#36	single
			1582.380	0.142	#14, 15	16
			1582.380	0.142	#2, 3	16
	Pier 2	Pier 4	953.618	0.134	#36	single
			953.618	0.134	#35	single
			953.614	0.140	#2, 3	16
			953.615	0.137	#14, 15	16
	Pier 2	Pier 0	230.031	0.141	#35	single
			230.032	0.140	#36	single
			230.030	0.142	#14,15	16
24 July 82	Pier 2	Pier 5	1582.383	0.139	#35	single
			1582.385	0.137	#2, 3	16
			1582.385	0.137	#14, 15	16
	Pier 2	Pier 4	953.614	0.138	#35	single
			953.617	0.135	#14, 15	16
			953.616	0.136	#2, 3	16
	Pier 2	Pier 0	230.027	0.145	#35	single
			230.031	0.141	#2, 3	16
			230.031	0.141	#14, 15	16
Mean Values	Pier 2	Pier 5		0.137	±0.005	
	Pier 2	Pier 4		0.136	±0.002	
	Pier 2	Pier 0		0.142	±0.002	
	Mean			0.138	±0.004	

1.3 AIRCRAFT PROBES

During the 1982 trilateration survey of the Gold River network simultaneous aircraft-flown temperature and humidity profiles were obtained with U.S. Geological Survey (USGS) and CGS sensor systems. The purpose of operating the two systems in parallel was to establish the credibility of the CGS system by comparing its temperature and humidity measurements with those from the time proven USGS system.

The USGS probe will be used as the standard for comparison, except in tests where mercury thermometers are used. The USGS probe has been tested by over 10 years of trilateration measurements, and a description of the system with a discussion of the precision of measurement made with this system may be found in Savage and Prescott (1975). Savage and Prescott give standard deviations of 0.1°C and 0.3 kPa for the mean temperature and water vapor pressure measured with the USGS probe.

Comparison of profiles flown during the 1982 survey show the CGS probes measuring systematically higher temperatures and lower humidities than the USGS probes. A change of about +0.2ppm in a distance measurement would result from these differences. Although this effect is small and only slightly greater than the error estimate for the USGS probe, the requirement for extremely precise measurements provides the stimulus for examining possible sources for these differences.

Temperature and humidity sensors for each system are installed within an open-ended, shielded, cylindrical

enclosure. The unit made up of the sensors, protective shield, and radiation shield is called a probe.

In the normal configuration a probe is placed on each side of the aircraft, mounted on a landing or wing strut, and orientated parallel to the long axis of the aircraft. Throughout the 1982 survey two probes from each system (a total of four) were attached to the aircraft.

During an EDM measurement the sensor equipped aircraft is directed along the optical path between the survey stations by observers at either end of the line. A data logger located within the aircraft periodically scans and records the sensor readings. The resulting temperature and humidity profiles along with end-point pressure readings are used to compute the refractive index which provides a scale correction to a measured length.

Accurate meteorological sensors are essential for a precise EDM distance measurements. This discussion will emphasize the assessment of temperature errors, since they are likely to contribute the greater part of the meteorological dependent error to a distance measurement. Error in the water vapor pressure, which is derived from the combination of humidity, temperature, and pressure readings, constitute a relatively smaller fraction of the total meteorological error budget.

Static air calibrations and wind tunnel tests were made in an attempt to isolate the cause of the temperature differences observed in the profiles. Results from these tests

are not definitive, but, generally, they show better agreement between the probe temperatures than that observed in the profiles. Lack of a reliable reference thermometer and the low maximum velocities limit the conclusions that can be drawn from the tests. It is beleived that the most likely source of the temperature difference observed in the profiles is due to the velocity dependent temperature correction, since tests under static or low speed conditions show good agreement or small differences opposite in sign from that observed in the profiles. The one test made in the field to determine the airspeed temperature correction for the CGS probe indicates a correction that is 1/3 of that used for the USGS probe and thus would increase the temperature difference to nearly 1°C.

1.3.1 TEMPERATURE MEASUREMENTS IN FAST AIRFLOWS

This discussion of possible errors in airborne temperature measurements is limited to evaluating instrumental error and the temperature rise experienced by a sensor within a probe placed in a fast air flow. The comparison of the two systems is not affected by path variations or by airspeed inaccuracy. The background material for this discussion is from a comprehensive review of airborne temperature measurements by Trenkle and Reinhart (1973).

Possible instrumental error include sensor calibration and scale error, recording error, self-heating error, response time error, and electric lead error. Sensor calibration and scale error may be assesed by laboratory comparison of the

sensor temperature readings with a temperature standard over the range of temperatures encountered under field conditions. Recording error may be evaluated by replacing the probe with a high stability circuit of known value. The self-heating error requires determining the current flow through the thermistor and the dissipation constant of the thermistor. The current causes Joule (I^2R) heating within the thermistor changing its temperature. The dissipation constant is defined as the amount of power required to raise the temperature of the thermistor 1° above the ambient temperature. It varies with the surface area of the thermistor and the medium being measured. In a thermally conductive medium such as a fast airflow, the heat is rapidly dissipated and the dissipation constant is about 1/10 of the value in still air. For a bead thermistor in a 5 m/sec airflow the dissipation constant is about 8 mW/°C (Omega, 1984). Provided that the current flow is low, no significant self heating will occur. The response time for a thermistor in a thermally conductive media is about 10 s or less (Omega, 1984), making response time error insignificant for the typical flown profile. The electric lead error is not generally considered important for high resistance thermistors.

The heating of the temperature sensor in a fast air flow is more difficult to assess. The physical characteristics of the sensor and probe determine the reduction in flow velocity and thus the proportion of the kinetic energy of motion converted to molecular motion. Complete conversion of the

energy of motion into thermal energy (a physical impossibility) will result in the full adiabatic temperature rise, ΔTk.

Assuming no addition or dissipation of heat, the full adiabatic temperature rise is experienced by a thermometer in the center of a container open only in the direction of flow. The full adiabatic temperature rise is given by the following equation (Trenkle and Reinhart, 1973, pg 33)

$$\Delta Tk = \beta(Vt)^2 \qquad (1.3.1)$$

where Vt = true airspeed (m/sec)

and $\beta = 1/(g \cdot J \cdot Cp) = 1/1987\ ^\circ C\ s^2/m^2$

where g= the gravitational acceleration of the earth

J= the mechanical equivalent of heat

Cp = the specific heat of air

The true airspeed, Vt , differs from that indicated by the aircraft pitot tube, Vi , by a density correction factor which is a function of the air temperature and pressure. That is

$$Vt = Vi \cdot T/288 \cdot 101.3/P$$

where T = absolute air temperature

and P = the total air pressure in kPa

The above equation assumes that the indicated airspeed is true at 288 K and 101.3 kPa. Use of the true airspeed in calculating the full adiabatic temperature rise is necessary because air is compressible.

To obtain the temperature of the unperturbed air, that is, the static temperature, Ts, the air temperature measured by the probe, Tm, is corrected by the proportion of the full adiabatic temperature rise recovered by the probe. The ratio of the probe temperature rise to the full adiabatic temperature rise is called the recovery factor, r, that is

$$r = \Delta Tkr/\Delta Tk$$

Which is used to obtain the desired relationship between the static air temperature and the measured air temperature.

$$Ts = Tm - r\Delta Tk = Tm - r\beta(Vt)^2 \qquad (1.3.2)$$

Assuming that the probe and the airspeed indicator's pitot tube are subjected to the same air flow velocity, only the recovery factor needs to be determined to compute the static temperature from the measured temperature and the true airspeed. For some geometric shapes, such as flat plates, r is a constant (Hinton, 1938) but for others r may vary with the velocity. We assume that r is approximately constant over the limited range of airspeeds used to fly the lines.

The recovery factor may be determined in the controlled conditions of a wind tunnel, or by field tests. Certainly, any results from wind tunnel tests should be confirmed by field test to evaluate possible variations due to probe location and orientation of the aircraft. The optimum tests, both in the wind tunnel and in the field, require a suitible reference thermometer. A total temperature probe, calibrated for recovery error, with a hermetically sealed platinum element of about 500 ohms is recommended by Trenkle and Rheinhart. With a well designed total temperature probe, r is very close to 1 and only the true airspeed needs to be measured to obtain the static temperature from the measured temperature (Stickney et al., 1981).

Lacking a suitible reference thermometer, the recovery factor may be estimated by comparing temperature readings over a range of velocities with the static air temperature from an independent source, or by assuming a linear change in the ambient temperature during the testing period.

1.3.2 PHYSICAL DESCRIPTION OF THE PROBES

The USGS probe contains two temperature sensitive resistors (thermistors) wired in parallel and a carbon coated humidity sensitive resistor (hygristor) mounted within the inner of two open-ended concentric cylindrical shields. The thermistors and hygristors used in the probe are manufactured by Viz Manufacturing Co. The 60 and 100mm diameter by 300 mm long cylindrical shields consist of phenolic plastic, chosen

for its nonconducting and insulating properties. Both the thermistors and hygristor are exposed to the direct air flow through the inner cylinder. The relation between the temperature and resistance of the thermistor is found by using three factory supplied calibration points to solve for the curve-fitting constants in the Steinhart-Hart equation (Omega, 1984)

$$1/T = A + B\ln R + C(\ln R)^3$$

where T = absolute temperature

R = the resistance of the thermister at T

A,B,C = curve fitting constants

For two Viz thermistors wired in parallel a change of +0.1° at 0°C results in a 40 ohm decrease in the resistance of the thermistor pair. At 30°C a change of +0.1° results in a 15 ohm decrease in the resistance. The electric lead error is likely to be less than 5 ohm and will not be a significant factor.

The resistance of the hygristor increases with increasing humidity, becoming very large under saturated conditions. In order to keep the resistance within a limited range, a 20k ohm resistor is connected in parallel with the hygristor.

The CGS probe contains a Weathermeasure HMP-15 temperature and humidity sensor. The rod shaped unit is mounted within the inner of two open-ended aluminum cylinders.

The HMP-15 contains a bead thermistor and a wafer capacitive type humidity element, both mounted on the tip of an 25 by 100 mm rod shaped housing. The sensors are protected by a screen with either 300 or 500 micron size openings. The filter cap is required in order to protect the humidity element from contamination by particulate matter. The separate battery powered readout unit has a switchable display and a linear 0 to 5 volt output corresponding to a temperature range of -5° to 45° and 0 to 100% relative humidity. The temperature (°C) and relative humidity corresponding to a measured voltage are given by

$$T = -5 + 10 \cdot (\text{temperature voltage})$$

$$\text{R.H.} = 10 \cdot (\text{humidity voltage})$$

1.3.2.1 Comparison of averages from profiles

Temperatures from the profiles recorded for the two systems contain no instrumental corrections. Factory provided calibration curves are used to convert sensor readings to temperature and humidity. The temperature readings for both types of probes are corrected for kinetic temperature rise using equation (1.3.2) assuming a recovery factor of 0.6. This is the value empirically derived for the USGS probe (Savage and Prescott, 1973). The recovery factor for the C.G.S. probe is not known. The tests made to determine the recovery factor for the CGS probe are inconsistant with the differences observed in the profiles, and for this reason it is not used.

Comparison of the average temperature differences from the profiles show the CGS probes measured 0.3°±0.04°C higher than the USGS probes. As seen in Figure 1.5, a plot of the average profile temperature difference, the observed temperature difference is constant over the range of temperatures encountered during the survey. A temperature difference of 0.3°C changes the refractive index scale correction by 0.3ppm resulting in an equal scale change in a measured distance.

Average relative humidity from the profiles differ by -11.1%±2.8%. As seen in Figure 1.6, the humidity difference appears to show a linear increase with increasing humidity. The humidity along with the air temperature and pressure is used to deduce the partial pressure of water vapor, which is fundamental in the calculation of the refractive index. Comparison of the two systems should, therefore, be made between the calculated value of the water vapor pressure not relative humidity. A plot of the water vapor pressure difference as a function of the USGS water vapor pressure is shown in Figure 1.7. The ppm change in the refractive index scale correction may be calculated by mutiplying the difference in mb by -0.4. In terms of the conditions encountered in the Gold River survey the observed humidity difference of 10% would change the refractive index less than -0.1ppm.

The net effect of the temperature and humidity differences is a relative change of +0.2ppm in the length of a

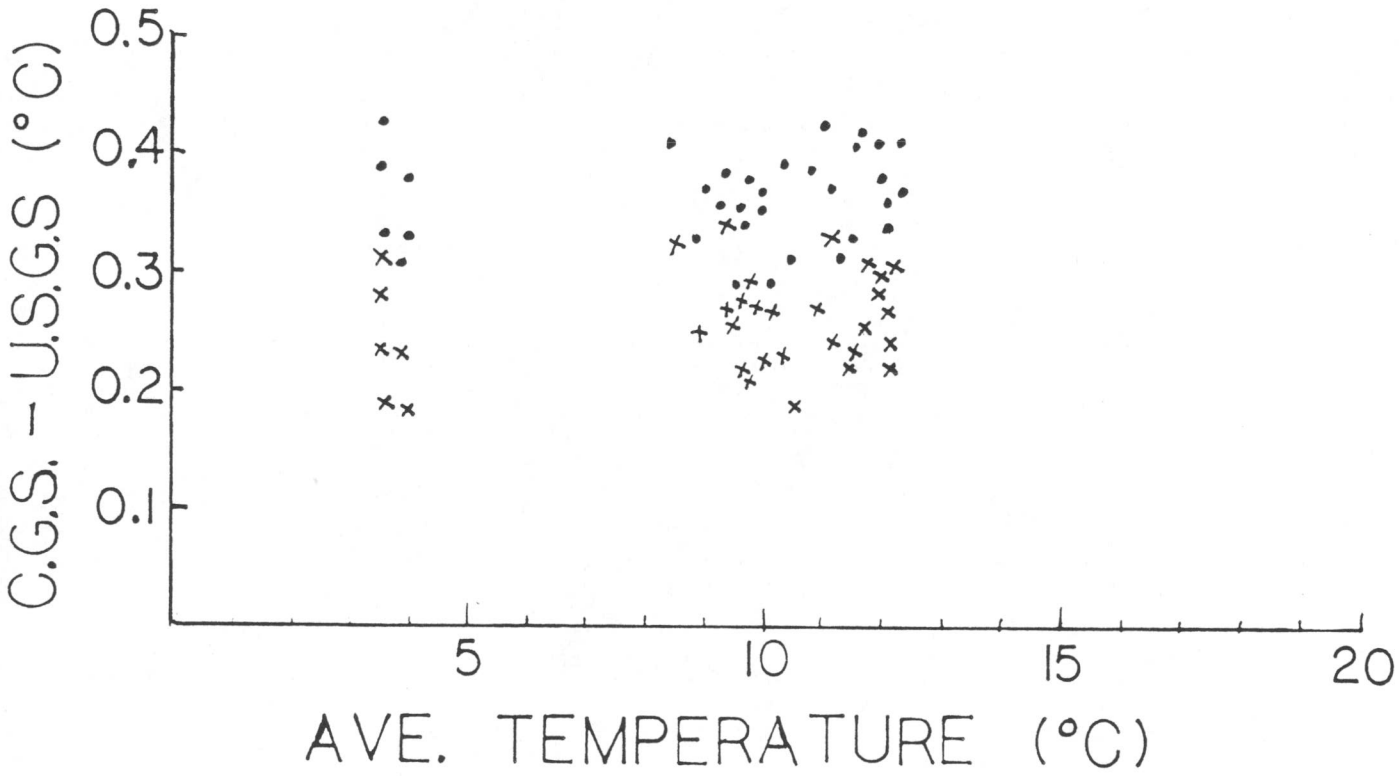

Figure 1.5. Temperature difference °C between averages obtained with the CGS and the USGS probes plotted relative to the USGS average temperature. Both systems are corrected for the kinetic temperature rise with a recovery factor of 0.6. The differences for the probes on the right side of the aircraft are shown with X's and dots are used for differences from probes on the left side. The probe ID'S are; USGS right 17, left 280; CGS right readout 1193, right probe 1851, left readout 1125, and left probe 1319.

line corrected with the temperatures and humidities measured with the CGS probe. Although the humidity difference was large, the low ambient temperatures encountered during the survey results in low water vapor pressures. Higher ambient temperatures would result in a larger water vapor pressure difference. However, under the worst circumstance, high humidity and high temperature, the difference in the water vapor pressure would result in less than a 0.4ppm change in a measured length.

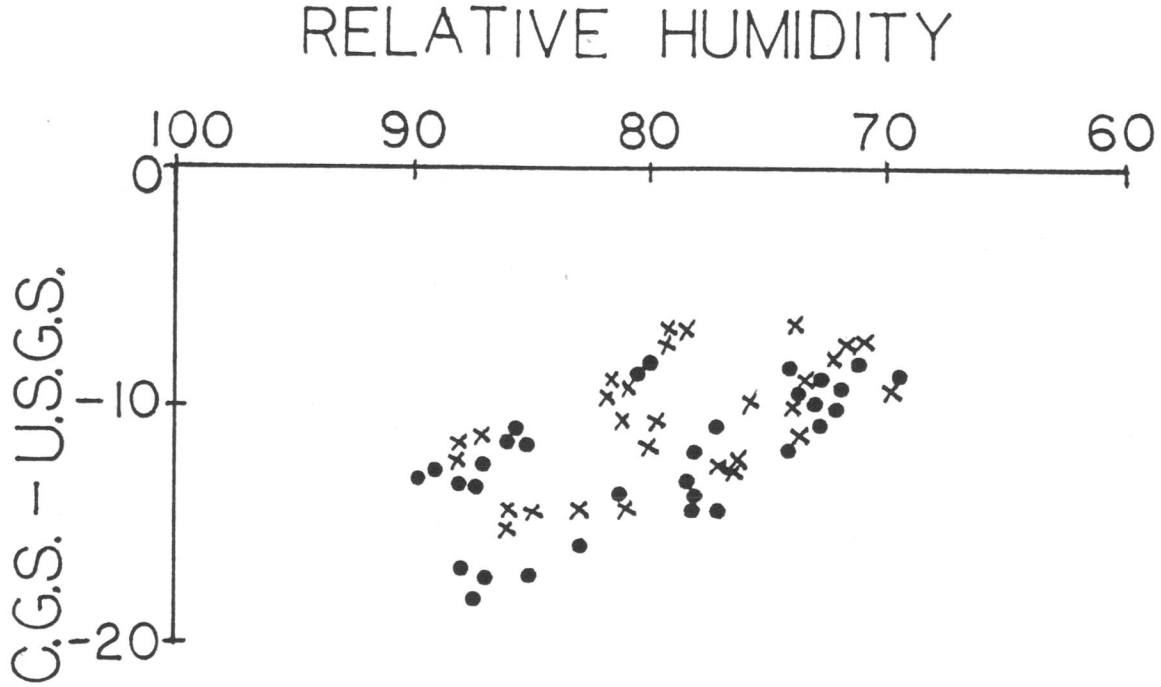

Figure 1.6. Relative humidity difference between averages obtained with the CGS and the USGS probes plotted relative to the USGS average relative humidity. X's are differences from the probes on the right side of the aircraft and dots are differences from the probes of the left side. Sensor ID's the same as in Figure 1.5.

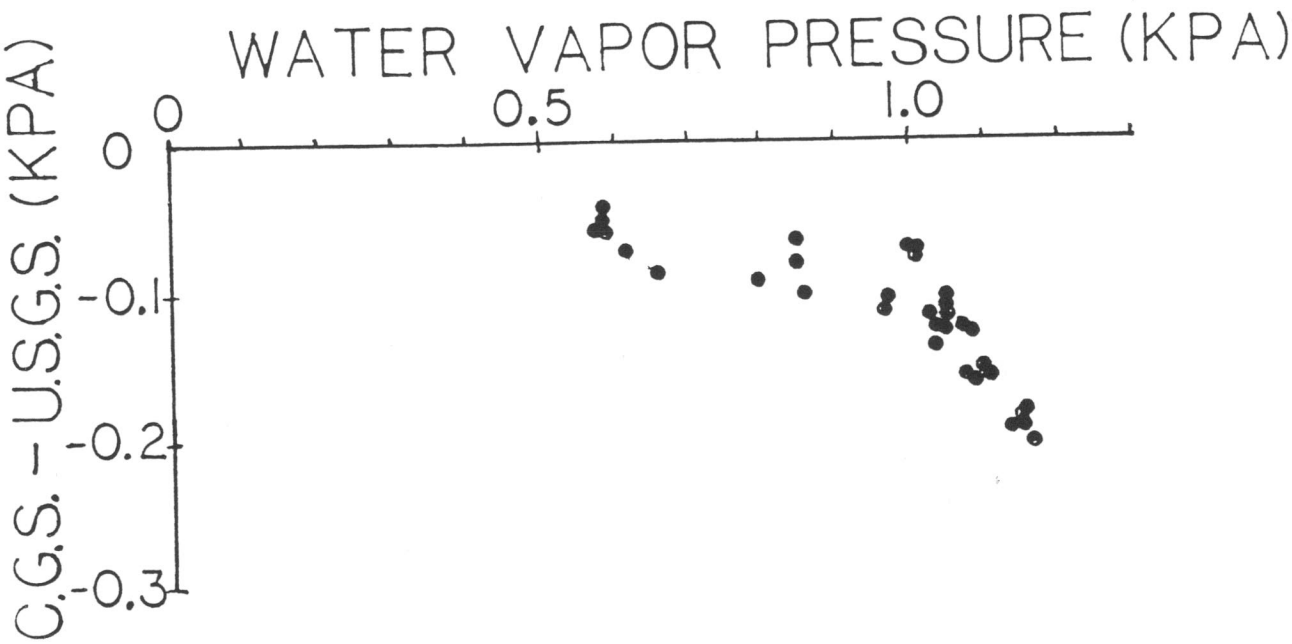

Figure 1.7. Computed water vapor pressure difference (kPa) between the CGS probes and the USGS probes relative to the average water vapor pressure measured by the USGS probes. The ppm change in the refractive index scale correction is 0.4 times the water vapor pressure difference in kPa.

1.3.2.2 Static calibrations

Temperature readings from the USGS and CGS temperature sensors were compared with an Hg thermometer in a temperature controlled airbath in an attempt to determine the scale and calibration error of the sensor. Results from the tests are disappointing and believed to be invalid, possibly due to a temperature gradient within the enclosure containing the sensors.

For the tests the sensors were extracted from the probes and sealed into a brass enclosure which was placed in a temperature controlled circulating water bath. The top surface of the enclosure was exposed to the air and an Hg thermometer was inserted into the enclosure from the top. Each time that the temperature of the water bath was changed a minimum of 30 minutes was allowed for the temperature in the water bath and the air within the enclosure to stabilize. At each temperature interval at least 3 readings of each sensor and the thermometer were made during a minimum interval of 10 minutes. The temperature difference between the sensors and the Hg thermometer are shown in Figure 1.8. The actual readings are listed in Table 1.5.

Table 1.5. Air bath temperatures

Time	C1 (k Ω)	°C	Displ left*	Volts	°C	Displ right*	Volts	°C	Hg
11:04	13.279	2.82	2.16	0.717	2.17	2.44	0.754	2.53	2.47
12.15	12.252	5.81	5.51	1.051	5.51	5.60	1.070	5.70	5.36
13:34	10.715	10.94	10.88	1.589	10.89	10.85	1.597	10.97	10.42
16:14	9.36	16.28	16.36	2.138	16.38	16.33	2.142	16.42	16.06
16:55	7.87	23.41	23.56	2.854	23.54	23.20	2.835	23.35	23.4
17:44	6.786	29.76	32.03	3.502	30.02	29.75	3.492	29.91	29.96
18:32	6.050	34.86	35.20	4.023	35.23	34.93	4.005	35.05	35.3
11:08	6.040	34.93	35.10	4.014	35.14	35.10	4.027	35.27	35.5
12:34	5.390	40.15	40.50	4.552	40.52	40.50	4.565	40.65	40.77
13:28	6.48	31.79	31.9	3.688	31.88	31.7	3.687	31.87	31.83
14:20	7.60	24.88	24.91	2.991	24.91	24.68	2.981	24.81	24.6
19:26	8.844	18.58	18.5	2.351	18.51	18.2	2.328	18.28	17.8

*left is the combination of Weathermeasure readout 1125 and probe 1319. right is the combination of readout 1193 and probe 1851.

The temperature differences (Hg themometer-probe sensor) are seen to be positive at low temperatures and negative at high temperatures with the crossover at about 30°C. The difference is as great as 0.5°C near 5° and 35°C. Repeated measurements at 5°, 10°, 15°, 25°, and 35°C show poor repeatablility with differences as large as 0.6°. The poor repeatability indicates some problem in the test procedures or in the equipment. The consistent agreement between the USGS and CGS sensors makes the Hg thermometer suspect. No explanation is offered to explain the anomalous Hg thermometer readings. Two plausible mechanisms, a temperature gradient within the air bath and a stem correction for the exposed part of the thermometer stem, would only increase the temperature difference.

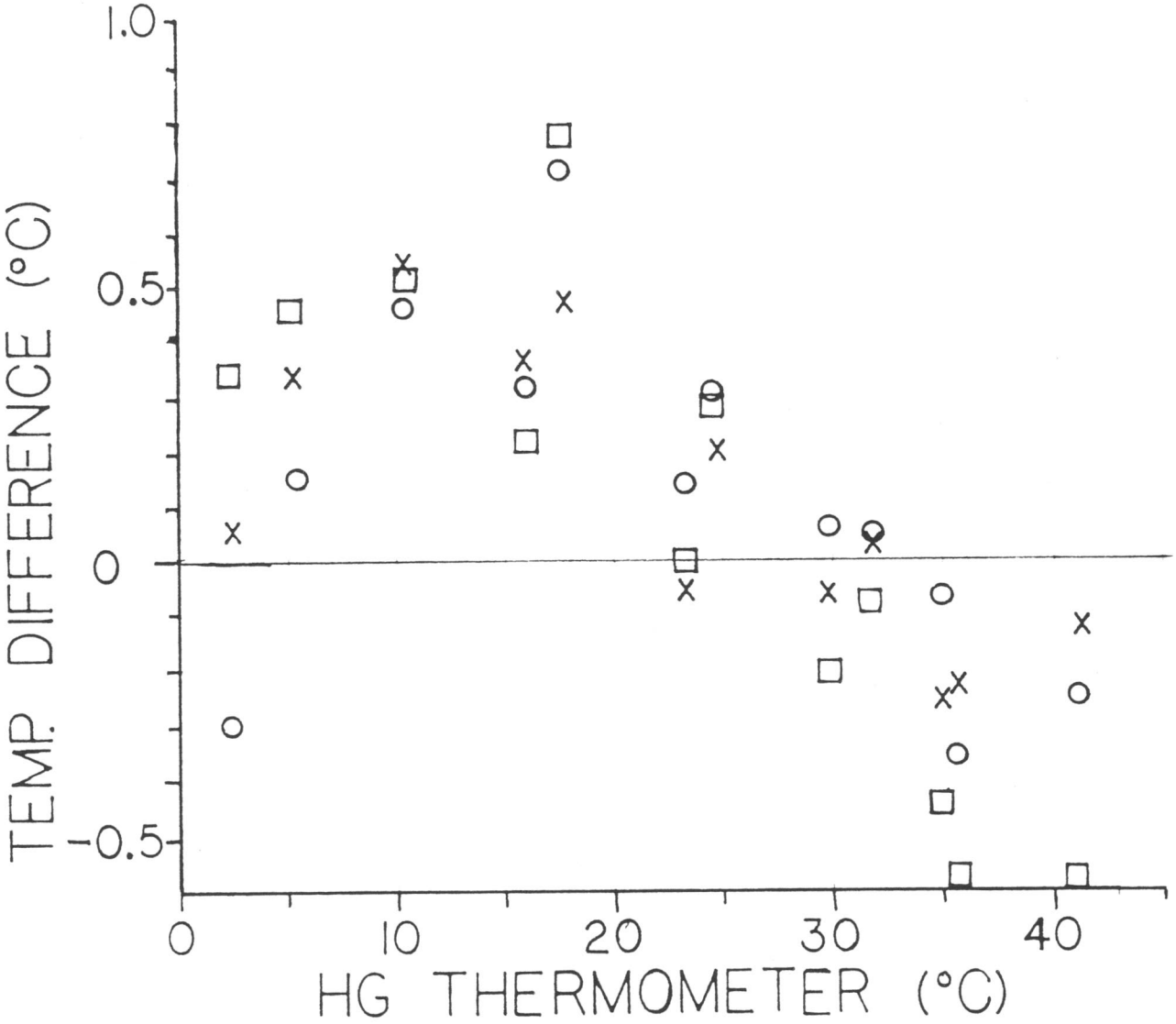

Figure 1.8. Air bath temperature differences between the probes' sensors and an Hg thermometer vs the Hg thermometer temperature. The square marks readings from USGS thermistor C1, the X's readings from the combination of CGS readout 1193 and probe 1851, and the O's readings from the combination of readout 1125 and probe 1319.

Discounting the Hg thermometer readings, the CGS sensors and the USGS thermistor are compared. This, of course, assumes that the sensors were not subject to the conditions that caused the Hg thermometer to err. Figure 1.9 shows the temperature difference plotted as a function of temperature. The plot shows the CGS sensors recording a linearly increasing temperature difference as temperature increases. Some of the differences are erratic, but the agreement is within about ±0.2° from 5° to 35°C. Between 4° and 10°C, the range of temperatures recorded during the Gold River survey, the temperature difference is negative. This is opposite of the difference observed in the average temperatures from the flown profiles.

The inconsistencies observed in the tests make the results unsuitable for determining the calibration and scale errors for the probes.

One positive result is the agreement between the temperature displayed by the Weathermeasure readout unit and that derived from the voltage output of the unit. These two values are nearly the same for the left probe, and differ by -0.1°C for the right probe.

1.3.2.3 Dynamic air temperature tests

Wind tunnel tests and a field test were made in an attempt to determine the the proportion of the full adiabatic temperature rise recovered by the CGS probe. The full adiabatic temperature rise is proportional to the

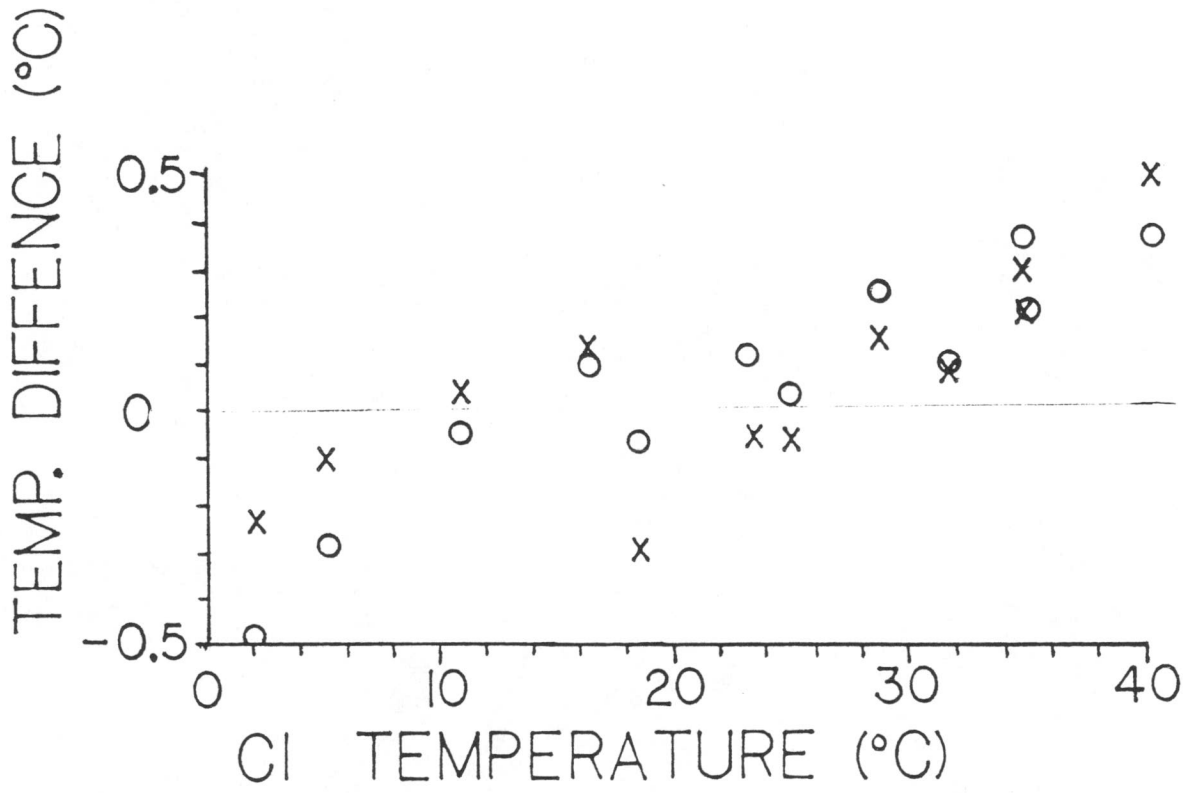

Figure 1.9. Air bath temperature differences between the CGS sensors and USGS thermistor C1. Symbols and ID's the same as in Figure 1.8.

square of the true airspeed, and the value is given by equation (1.3.1). A plot of the temperature rise as a function of true airspeed for recovery factors of 1.0 and 0.6 are shown in Figure 1.10.

To determine the recovery factor, both the temperature of the unperturbed air, that is, the static temperature, and the true airspeed must be known. Using a recovery factor of 0.6, the value empirically determined for the USGS probe, velocities greater than 15 m/s are needed to give a temperature rise of 0.1°C.

Tests in the wind tunnel at U.B.C. were limited to a maximum airspeed of 23 m/s. At this velocity the temperature rise in a probe with a recovery factor of 0.6 is 0.15°C. Thus, velocities are not adequate to determine the recovery factor, but they do provide another temperature comparison between the sensor systems and the Hg thermometer.

The tests were made in a wind tunnel with a cross sectional area of $\simeq$16 m^2. A probe provided by the USGS and a CGS probe, a Hg thermometer, and a pitot tube were mounted near the center of the wind tunnel. The thermometer was placed on the insulated lee side of the mounting support for the probes and was read through a pair of binoculars. The true airspeed was calculated from manometer readings of the pitot tube. The results from the tests plotted as temperature difference between the sensors and the Hg thermometer as a function of true

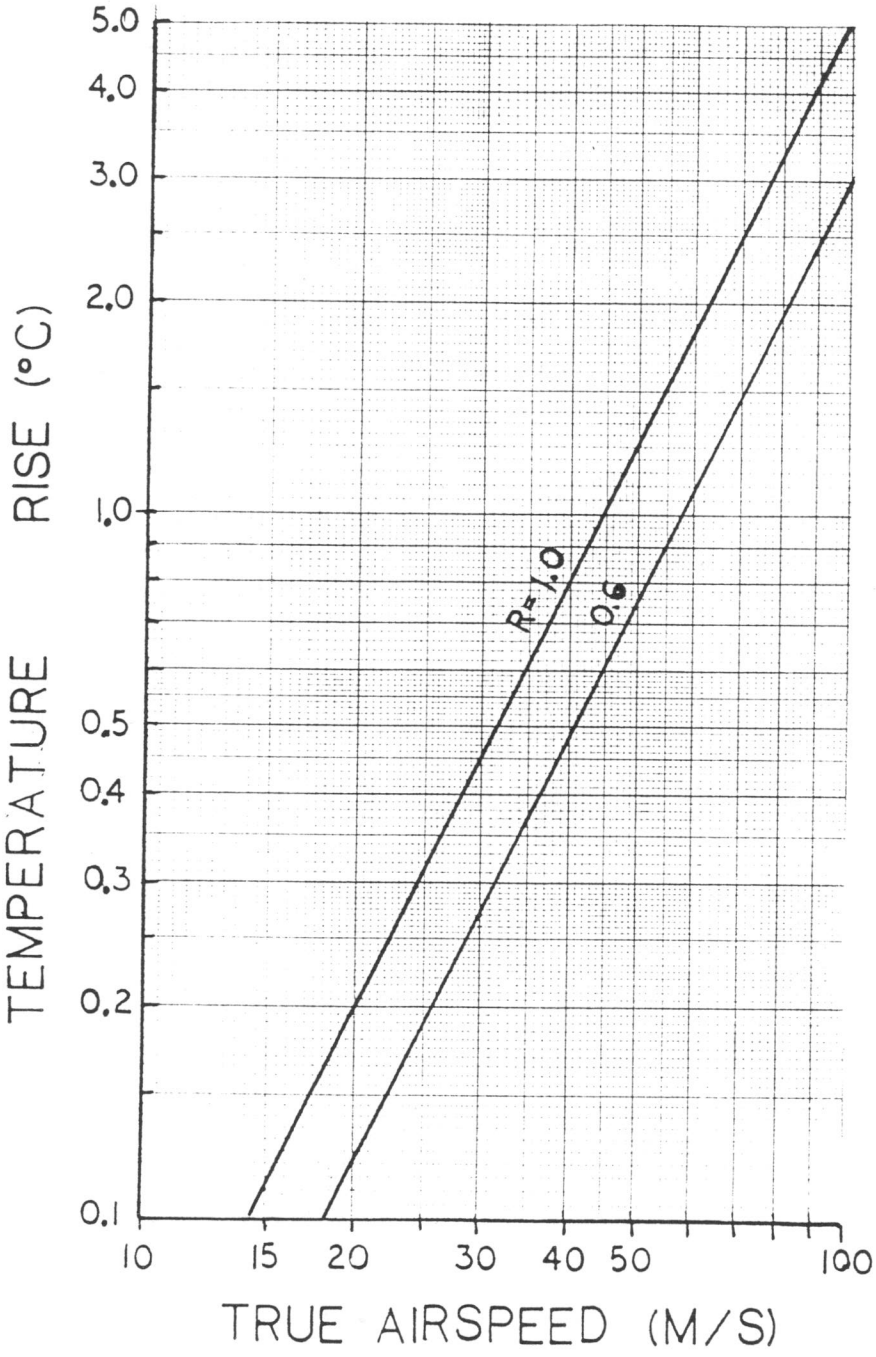

Figure 1.10. Kinetic temperature rise for recovery factors of 1.0 and 0.6 vs true airspeed in m/sec.

airspeed are shown in Figure 1.11.

Over the entire range of airspeeds there is good agreement between the sensors and the Hg thermometer. The sensors diverge from the theoretical temperature rise assuming a recovery factor of 0.6 at the higher velocities, but because the difference is less than the possible reading error for the Hg thermometer this is inconclusive. Another possibility is that at low velocities r is different from the value at higher velocities. This might be expected if the flow regime changes from laminar to turbulent at the higher velocities, as there would be extra dissipation of energy in turbulent flow (Hilton, 1938).

A field test was made to determine the recovery factor for the CGS probe. Wet and dry bulb temperature measurements were made on a lookout tower to provide the static air temperature, and temperature and humidity readings were made as a probe equipped helicopter flew over the tower. Only a limited range of airspeeds (45 - 54 m/s) were used during the test. Using equation (1.3.2) the recovery factor may be computed from the static temperature, probe temperature, and the true airspeed.

The recorded data and the corresponding computed recovery factors computed using equation (1.3.2) are shown in Table 1.6. The average value for the recovery factor from thes tests is $0.20 \pm 0.18 °Cs^2/m^2$. Any recovery factor for the CGS probe lower than the value of 0.6 will

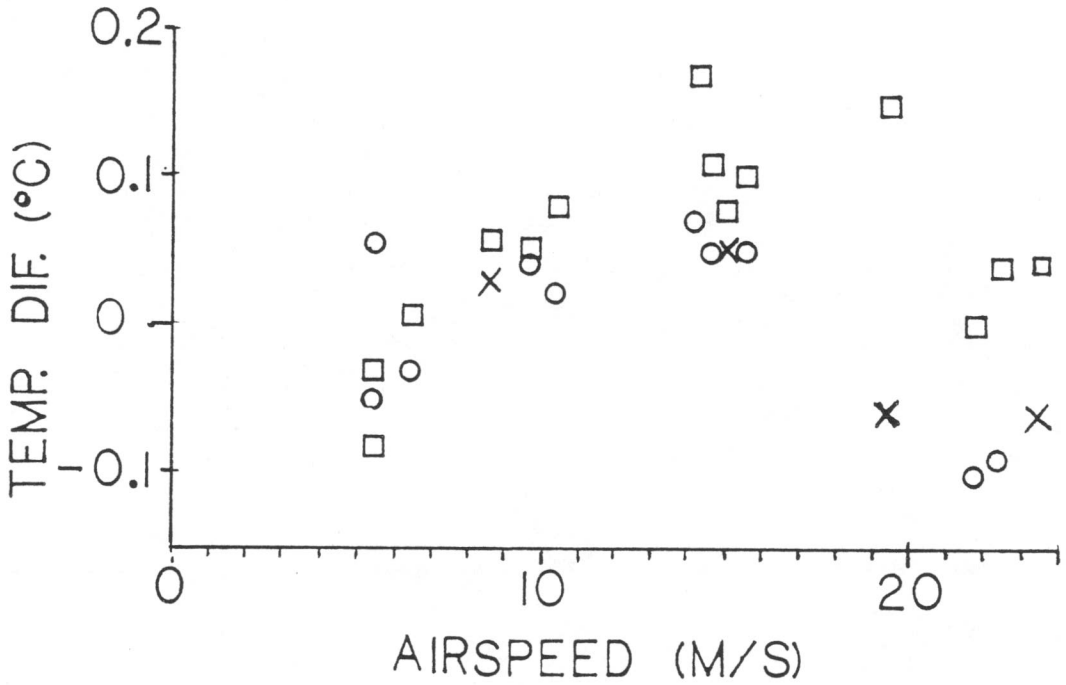

Figure 1.11. Temperature difference between probes and an Hg thermometer as a function of the airspeed in the UBC wind tunnel. Symbols and ID's are the same as in Figure 1.8. Estimated reading error for the Hg thermometer is 0.1°C

increase the temperature difference seen in the comparison of the profiles (Figure 1.5). This fact and the uncertainty of the average recovery factor make the results suspect.

The humidity measurements, however, agree well with the differences observed in the profiles (Figure 1.6). During the tower tests the CGS probe consistently measured the humidity about 10% lower than the value calculated from the wet and dry bulb readings in the tower.

Table 1.6. Metcalf tower probe calibration

Tower Dry (°C)	Wet (°C)	Comp. Hum %	Probe Temp (°C)	Probe Hum %	Airspeed (m/s)	Recovery Factor
18.4			18.5		54	0.1
18.9			18.8		54	0.1
18.9			18.7		51	0.2
18.5			18.8		53	0.2
18.1			18.6		54	0.3
18.4			18.8		54	0.3
18.7			18.6		49	-0.1
18.7			18.6		49	-0.1
18.5	16.8	84	18.6	71	49	0.1
18.8	16.8	82	18.8	72	41	0.0
18.3	16.5	83	18.8	72	50	0.4
18.3	16.5	83	18.9		49	0.5
18.4	16.6	83	18.7	72	45	0.3
18.7	16.7	82	18.8	72	45	0.1
18.7	16.7	82	18.7	72	44	0.0
18.4	16.6	83	18.8	72	45	0.5
18.4	16.6	83	18.8	72	45	0.4
18.7	16.7	82	18.9	72	45	0.2
18.9	16.8	81	19.1	71	53	0.1
18.7	16.7	82	19.2	70	54	0.4

1.4 PRESSURE

The average refractive index used to correct a measured length is obtained from an integrated average of the refractive index at the "midpoint" of adjacent temperature-humidity readings. The air pressure readings are not made by the aircraft flying the line, instead they are calculated from the pressure at the instrument end of the line. The procedure uses the total air pressure readings at the instrument station, the station elevations, the estimated beam curvature, and the temperature and humidity profiles to construct a profile of the air

pressure. The deatails are available on request. Pressure readings made at the reflector end of the line are not used in the refractive index calculation, but only as a check on the calculated value. Difference between the observed and calculated pressure at the reflector end may arise from imprecise station elevations, as well as instrumental error at either end. A change of 10 m in the relative elevation difference results in a 0.3ppm change in a measured length. For this reason, the value of the station elevations used to reduce repeated surveys should be checked for consistency.

During the 1982 Gold River survey pressure readings at the instrument end of a line were made with two Bell and Howell Model 4-461 digital pressure transducers, and a Wallace and Tiernan FA-181 0-7,000 ft altimeter. Pressure readings at the reflector end were made with a Wallace and Tiernan altimeter. The mean of corrected readings taken at the beginning, middle, and end of each line measurement was used in the refractive index calculation.

Corrections for the pressure instruments were obtained from calibrations performed by the Division of Mechanical Engineering of the National Reseach Council in April of 1982. Calibration curves for the pressure instruments used in the Gold River survey may be obtained from the C.G.S.

At the end of each day that distance measurements were made in the Gold River survey, the pressure instruments were compared in the motel room. These measurements are listed in Table 1.7. They show good agreement in the measured pressure,

with the spread of all readings being less than 0.03 inch or 0.9 mb in any given day.

Table 1.7. Motel pressure readings

Date mo/da	B&H #2145	B&H #2130	Alt #59-13	Alt #301038	Alt #765
7/15	29.55	29.57		29.58	
7/17	29.49	29.52	29.55	29.55	29.54
7/18	29.59	29.61		29.63	29.62
7/19	29.60	29.59	29.62	29.62	29.61
7/20	29.59	29.61		29.61	29.61
7/21	29.79	29.79	29.85	29.81	29.80
7/22	29.97	29.97		29.99	29.99

All reading given in inches of Hg, ie, the units of the B&H transducers.

Field measurements are also used to compare the instruments. Table 1.8 lists actual and corrected pressure readings at the instrument and reflector, and the calculated reflector pressures corresponding to the instrument pressure readings. As seen in the table, the altimeter pressures at the instrument and reflector agree well with corresponding readings from B&H transducer #2130. Pressures from B&H transducer #2145 are generally about 0.03 inch lower than that from the other barometers. For that reason , the pressure used to reduce the measured lines is that from #2130, not the mean of #2130 and #2145.

The agreement between the calculated and measured pressure at the reflector indicates that relative elevation control is good and that the algorithm used to calculate the pressure profile provides a good approximation of the actual pressure.

Table 1.8. Observed and calculated pressures

Line *	Date mo/da	Instrument station B&H #2145	B&H #2130	alt #765	Reflector station alt #30138	Calc. #2145	Calc. #2130
1	7/17	24.72	24.73	24.77	25.33	25.34	25.35
2	7/17	24.73	24.77	24.77	24.33	24.29	24.33
3	7/17	24.74	24.77	24.77	24.37	24.33	24.37
4	7/17	24.75	24.78	24.78	24.40	24.37	24.39
5	7/17	25.33	25.37	25.36	24.32	24.30	24.32
6	7/18	25.33	25.37	25.37	24.38	24.35	24.39
7	7/18	25.33	25.37	25.38	24.41	24.37	24.41
8	7/18	25.35	25.38	25.39	25.41	25.37	25.40
9	7/18	25.35	25.39	25.40	26.48	26.43	26.47
10	7/18	25.36	25.40	25.40	26.29	26.25	26.28
11	7/18	24.79	24.82	24.82	26.29	26.26	26.29
12	7/18	24.78	24.81	24.81	26.48	26.44	26.46
13	7/18	24.77	24.79	24.81	26.09	26.04	26.07
14	7/18	24.77	24.79	24.80	25.41	25.37	25.39
15	7/20	24.32	24.35	24.35	24.33	24.30	24.33
16	7/20	24.26	24.28	24.29	24.33	24.31	24.33
17	7/20	24.27	24.30	24.30	24.36	24.33	24.36
18	7/22		25.62	25.62	24.61		24.61
19	7/22		25.64	25.64	26.33		26.33
20	7/22		25.66	25.65	26.73		26.74
21	7/22		25.64	25.64	26.53		26.52
22	7/22		26.69	26.71	26.50		26.50
23	7/22		26.69	26.69	26.29		26.30

All reading given in inches of Hg the units of the B&H transducers.
* Line number refers to the sequential order that observations were made during the Gold River survey.

1.5 ESTIMATE OF THE ACCURACY AND PRECISION OF A DISTANCE

The theoretical error in a distance measurement may be estimated from the contributions to the constant and scale error. The major components of the constant error are pointing error, zero error, non-linearity in the phase detector, receiver noise, zero-crossing error due to signal level, and centering. Scale error results from short and long term drift in the modulation frequency and error in the calculated mean

refractivity.

1.5.1 CONSTANT ERROR

It is assumed that pointing error is not a factor in long line measurements, and that error from the zero crossing detector is minimized by careful adjustment of the signal level during range measurements. No tests were made to determine the non-linearity in the phase detector, so use is made of the value of ±5 mm provided by the manufacturer. Zero error, or error in the instrument and reflector constants, is estimated from the standard deviation of the Victoria baseline measurements to be ±4 mm. Receiver noise (see section 1.2) is given by Berg et al (1981) to be ±2 mm. Extreme care taken in centering both the instrument and reflectors reduce centering error to less than 0.5 mm. Assumming that these error are random, the theoretical constant error is

$$\sigma = \sqrt{[(5\ \text{mm})^2+(4\ \text{mm})^2+(2\ \text{mm})^2+(0.5\ \text{mm})^2]} = \pm 6.7\ \text{mm}$$

Careful calibration might reduce the contributions of non-linearity and zero error to as little as 1mm.

1.5.2 SCALE ERROR

The tests of the short term stability reading of the long term stability of the modulation frequency show drift less than 0.5ppm. Error in the average refractivity arise from temperature, water vapor pressure, and pressure error. The

partial derivatives of the group refractive index with respect to the desired meteorological parameter defines the error limits on the measurement for a desired accuracy. Savage and Prescott (1973) estimate 0.1°C and 0.3 kPa for the standard deviation of the mean temperature and water vapor pressure for atmospheric profiles measured with the USGS probe. The resulting scale error in a distance is 0.1ppm due to temperature and 0.1ppm due to the water vapor pressure. The standard deviation in the average pressure is estimated to be 0.03 kPa (0.01 in Hg) from the agreement between the altimeter and B&H digital barometers. It is noted, however, that the B&H units differed by as much as 0.12kPA (0.04 in Hg) during the Gold River survey, but this difference is attributed to malfunction of one of the units. The resulting theoretical scale error for lines reduced with the USGS probes assuming random values for the components is

$$\sigma = \sqrt{[(0.1\text{ppm})^2 + (0.1\text{ppm})^2 + (0.1\text{ppm})^2 + (0.1\text{ppm})^2]} = \pm 0.2\text{ppm}$$

The scale error using the CGS probes is not well defined. The uncertainty about the airspeed correction makes any comparison with the USGS probes tenative. In addition, the linearity and stability of the circuitry used to condition the output of the Weathermeasure probe has not been tested. The absolute temperature calibration for the probe is not known, but the agreement with the USGS thermistor in the U.B.C. wind tunnel suggest that at room temperature it is within the 0.1°C

error of the USGS thermistor. If we assume the airspeed correction for the CGS probe is the same as that used for the USGS probe, the average temperatures from the simultaneous profiles differ by 0.3°C. A reasonable estimate for temperature error for the CGS probe is 0.2°C, with the resulting scale error being 0.2ppm. The difference in the average water vapor pressure from the simultaneous profiles is less than 0.3 kPa, that is within the error of the USGS probe. It is reasonable to assume that the scale error is similar to the 0.1ppm given for the U.S.G.S. probe. Taken together the estimated theoretical standard deviation in the scale correction for lines reduced with the CGS probes is

$$\sigma = \sqrt{[(0.2\text{ppm})^2+(0.1\text{ppm})^2+(0.1\text{ppm})^2+(0.1\text{ppm})^2]} = \pm 0.26\text{ppm}$$

Combining the constant and scale error, the theoretical standard deviation of a distance reduced with the USGS probe is then estimated to be

$$\sigma = \sqrt{[(6.7\text{ mm})^2+(0.2\cdot 10^{-3}\cdot \text{Dist(m)})^2]}\text{ mm}$$

For distances reduced with the CGS probe we would increase the scale error to $0.26\cdot 10^{-6}$. The estimate for the CGS probe may not represent the true error.

The residuals obtained from the adjustment for station positions provide an estimate for the precision of a measurement, but yields no information concerning the accuracy

of the survey. If we include only lines with aircraft flown refractivity scale corrections and weight all measurements equally the residuals give 5 mm as the standard deviation of a length. With an average length of 24 km, 5 mm is less than the estimated theoretical error of 8.3mm. However, the theoretical error must be modified to make the comparison valid. The zero error is eliminated by assuming no change in the instrument or reflector constants during the survey. In addition, for a group of lines with random lengths the linearity error would be reduced to ≃2.5 mm, since some lines will have no correction while others will have a 5 mm correction. The resulting standard deviation for a 24 km long line is 5.8 mm, which compares favorably with that obtained from the adjustment.

1.6 RECOMMENDATIONS

Distance meter

1. The following simple field tests described by Berg et al. (1981) to check the instrument sensitivity, the zero-crossing detector, and the pointing error should be made to verify instrument operation.
   a. To test instrument sensitivity, place an ND6 neutral density filter on the collimator, and range to a single reflector at short range. (Take note of the maximum signal meter deflection for future reference.) When sensitivity is normal, it should be possible to obtain ranges.

b. To test the zero-crossing detector, take measurements at the upper and lower limits of acceptable signal level as indicated by the panel meter. A span of more than 5 mm indicates a need for readjustment of the zero-crossing detector.

c. To test the pointing error, the returned beam is rotated through six positions in the receiving optics, and the distance measurements compared. The position of the returned beam may be found by inserting a piece of paper in front of the receiver. If the span of the measurements is less than 10 mm, it may reasonably be assumed that handling during transportation has not caused optical misalignment.

2. The instrument calibration at the Victoria baseline should include measurments for the linearity. This requires establishing a linearity baseline of 10 monuments spaced 1 m apart. In addition, more of the distances in the baseline should be observed. To reduce refractivity error the baseline rangings should be made, if possible, on overcast, light or moderately windy days.

3. All baseline calibrations should be made to a calibrated single reflector and mount. All other reflector-mount constants are referenced to this standard. This allows separation of the instrument and reflector constants. The physical arrangement of the reflectors in the 16-reflector mount makes its use on short baseline calibrations difficult, since at least two of the center positions have

to be filled to obtain axial symmetry.

4. The drift in the modulation frequency should be tested under adverse field conditions.

Probes

Although the Weathermeasure probe provides an easily measured voltage output, the uncertainty in the calibration, airspeed correction, output linearity, and response time delay require a series of tests if its use is to be continued. It is recommended that:

1. The voltage output from the Weathermeasure probe be checked over a range of battery voltages and ambient temperatures. The calibration box provides a convenient constant input.
2. The response time delay of the filter tipped probe may not be insignificant. The response time delay should be measured with the filter caps on and off, and care should be taken to insure that the filters are not plugged.
3. The velocity related temperature rise needs to be determined. Several options are available. The method favored is to make simultaneous measurements with a total temperature thermometer as recommended by Trenkle and Reinhart (1973). These thermometers are relatively expensive, ≃$2000, and they require very accurate resistance measurements. They do, however, provide an absolute and stable reference. They are compact and a

model exists that isolates the temperature sensor from water droplets or particulate matter in the air (see Stickney et al, 1981, for additional information). It may be possible to replace the platinum temperature element with a thermistor, eliminating the need for extremely accurate resistance measurements. Alternatively, the CGS probes could be calibrated by Rosemount Inc. or some other agency with experience in making temperature measurements in fast air flows. This, of course, will not provide any information on the effect of mounting location on various aircraft. Berg et al (1981) use slightly different airspeed corrections for different models of helicopters.

4. The influence of airspeed on the humidity reading needs to be assessed. The CGS probe measured the relative humidity about 10% lower than the USGS probe in the profiles (Figure 1.6) and the same amount lower in the Metcalf tower tests (Table 1.6).

Other alternatives to the above tests are to use a U.S.G.S. design probe, or to build a probe incorporating a Rosemount total temperature thermometer. Use of the Rosemount thermometer would eliminate the uncertainty in the airspeed correction, increase the long term stability, and reduce the size of the externally mounted equipment. Use of the USGS probe complicates the recording and reduction of of the readings, but its stablility is proven.

Pressure

1. A pressure reference standard that stays in the motel room should be used to compare the pressure devices at the end of the working day. This standard should be calibrated frequently with an Hg barometer, or some other pressure reference device.
2. There are several types of portable pressure devices that are as accurated as the B&H digital barometer but are more transportable and field worthy. These include, for example, a voltage output pressure transducer by Setra Systems and a frequency output pressure transducer by Paroscientific. The policy of using altimeters to check the pressure readings should be continued.

1.7 STRAIN RESOLUTION

Remeasurement of a trilateration network can be used to determine deformation within the area covered by the network. The relative displacement of stations within the network results in a change in the distance between the stations. The ratio of the change in the length of a repeated distance measurement to its length defines its extension. The extension of a line with the approximate azimuth θ (measured clockwise from north) is related to the surface strain tensor increments $\epsilon(k,l)$ through the tensor transformation law

$$e = \epsilon(k,l)\beta(k,l)\beta(l,k)$$

where $\beta(k,l)$ are the direction cosines of the line relative to

a geographic coordinate system with the 1 axis oriented to the east and the 2 axis oreinted to the north. The full expression of this equation for e(i), the extension of the ith line with azimuth $\theta(i)$ is

$$e(i) = \epsilon_{11}\sin^2\theta(i) + 2\epsilon_{12}\sin\theta(i)\cos\theta(i) + \epsilon_{22}\cos^2\theta(i)$$

Three or more repeated measurements will determine the average strain increments ϵ_{11}, ϵ_{12}, and ϵ_{22}. Assuming uniform strain in a network containing N repeated measurements with the standard deviation of an extension being σ, the standard deviation in ϵ_{11} and ϵ_{22} are about $\sigma\sqrt{(4/N)}$ and the standard deviation in ϵ_{12} about $\sigma\sqrt{(2/N)}$ (Savage, 1983). Since two surveys are being compared, systematic error due to miscalibration of the instrument and meteorological sensors may result in an systematic constant or scale length change. A systematic error between two surveys would impose a dilatational strain upon the derived strain field proportional to the error in the extensions. The standard deviation of the normal components ϵ_{11} and ϵ_{22} would need to be increased to compensate for such an error, but any calculated shear strain will be unaffected. That is, the imposed dilatation does not affect the angle changes between surveys.

Assuming no systematic error, the standard deviation of a measured extension for an average line (24 km) in the Gold River network is 8.2 mm or 0.5ppm [i.e. $\sqrt{2}$ times the standard deviation of an individual measurement given by equation

(1.5.1)]. Assuming uniform strain, the strain resolution of the Gold River network is estimated by the above formulas to be 0.2 μstrain in the normal strains and 0.15 μstrain in the tensor shear strain. The detectable limit at the two standard deviation level of the rate of strain accumulation under the most favorable circumstances is 0.4 μ strain per year. If the deformation of the network is reasonably uniform in time, a resurvey after 2 years will resolve the rate of strain accumulation at the 0.2 μstrain level, and after 5 years at the 0.1μstrain level. A typical rate of strain accumulation in tectonically active areas is 0.2 μstrain per year (Savage, 1983). As will be shown in the discussion of the comparison of the 1982 and 1947 surveys of the Gold River network, the rate of strain accumulation appears to be at or below 0.2 μstrain per year. A resurvey of the Gold River network after a five year interval should clearly define the pattern of strain accumulation in this area.

2. 1947 TRIANGULATION

Baseline measurements for the Gold River network consist of a triangulation survey made by Slocomb and Swinnell of the B.C. Ministry of Surveys in 1946 and 1947. The angles were probably observed with a 1" direction theodolite but the observing procedure are not known (Wilkenson, 1983, personal communication). The field notebooks provide information about the number of sets per angle, the spread of the readings, and sketchy notes about the type of targets sighted. It appears that the typical angle measurement consists of 10 sets of forward and reverse pointings made between two stations. Angles appear to be measured individually, rather than in a round. Both targets and cairns were sighted, and observations were apparently made during the day.

The subset of the 1946-47 triangulation survey including all the monuments tied to the 1982 trilateration survey is shown in Figure 2.1. This subset consists of 57 angles between 10 stations. An abstract of the observed angles taken from the field notebooks is given in Table 2.1. Most of the angles listed were directly observed, but because the survey includes several stations outside of the Gold River network some are derived from the sum or difference of sightings to an intermediate station.

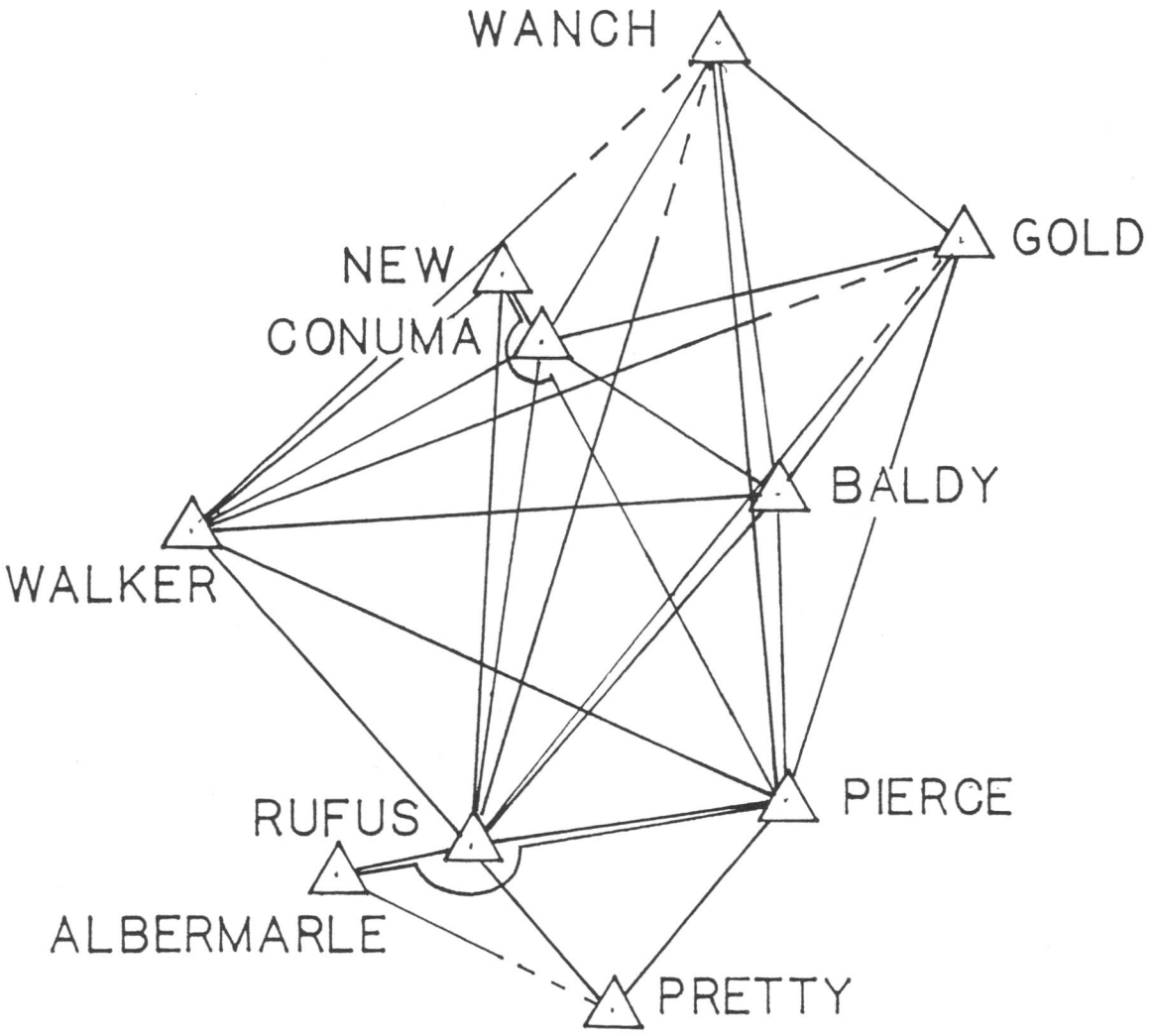

Figure 2.1. Sketch showing directions enclosing horizontal angles observed by the B.C. Ministry of Surveys during the 1946-47 triangulation survey. The solid lines shows the directions observed from both stations and the dashed line the station observed from one end only.

Table 2.1. 1947 Triangulation

OBS STA	STA 1	STA 2	ANGLE ° ' "	SETS	SPREAD (s)	σ (s)	CHANGE 82-47
Alber	Rufus	Pretty	36 37 42.310		15	5.0	-1.4
Baldy	Pierce	Rufus	45 04 18.510		17	5.1	5.1
	Rufus	Walker	44 59 07.110		9	2.6	1.1
	Walker	Conuma	33 44 28.510		22		-0.6
	Conuma	Wanch	49 36 26.410		17	6.4	-3.0
	Wanch	Gold	44 51 28.710		18	6.3	-2.0
	Gold	Pierce	141 44 09.510		16	5.4	-3.6
	Conuma	Gold	94 27 52.810		11	4.2	1.7
Conuma	Wanch	Gold	47 30 11.710		10	3.2	-0.6
	Gold	Baldy	45 07 54.810		18	6.0	1.8
	Baldy	Pierce	29 03 14.610		17	4.7	0.8
	Pierce	Rufus	38 12 08.510		17	5.4	-1.8
	Rufus	Walker	54 58 25.810		14	4.5	-0.8
	Walker	New	92 18 27.110	/5*	9/5*		**
	Walker	Wanch	145 08 12.210	/10	12/9	5.2	**
Gold	Pierce	Baldy	18 51 53.0	5	3	1.2	
	Baldy	Conuma	40 24 10.510		12	4.7	0.3
	Conuma	Wanch	52 43 46.810		15	4.5	-6.8
New	Conuma	Walker	75 40 15	5	8		**
	Pierce	Rufus	32 54 42.8	7	25		**
	Rufus	Walker	47 29 01	5	8		**
Pierce	Pretty	Alber	42 16 22.910			4.6	2.8
	Pretty	Rufus	42 59 16.910			3.9	-1.1
	Rufus	Walker	32 03 40.610		12	4.6	2.8
	Walker	Conuma	35 40 42.010		7	2.5	1.0
	Rufus	Conuma	67 44 24.410		10		-3.0
	Conuma	Baldy	27 08 48.510		9		-0.9
	New	Baldy	26 23 14.0	5	11		**
	Baldy	Gold	19 24 01.810		12		-1.0
	Conuma	Wanch	23 09 15.410		12		2.0
	Wanch	Gold	23 23 31.110		10		-2.0
Pretty	Rufus	Pierce	80 21 35.610		12	4.5	-1.5
Rufus	Alber	Walker	59 14 59.2	5	17		**
	Walker	New	44 29 42.6	5	11		**
	Walker	Conuma	49 01 31.510	/10	9/14		3.0
	Walker	Pierce	123 05 05.4			6.1	-3.2
	Conuma	Wanch	8 19 43.810	/10	14/15		-0.9
	Conuma	Gold	31 18 10.110		15		0.4
	Conuma	Baldy	34 01 02.910		12	3.8	-0.9
	Baldy	Pierce	40 02 30.110		19	5.0	-4.2
	Gold	Pierce	42 45 12.810		16		4.5
	Pierce	Pretty	56 39 10.910		12	4.8	0.3
	Pretty	Alber	121 00 54.010	/10	13/14	6.3	-4.4
	Alber	Pierce	182 19 56.010	/10	11/17		3.3
Walker	Wanch	Conuma	16 36 17.710		13		-6.7
	Wanch	New	4 34 56.010	/5	7/17		**

TABLE 2.1 cont.

OB STA	STA 1	STA 2	ANGLE ° ' "	SETS	SPREAD (s)	σ (s)	CHANGE 82-47
	Conuma	Rufus	75 59 59.210		13	3.8	2.6
	Conuma	Pierce	51 08 45.215		20		1.6
	Conuma	Baldy	24 01 45.515		27		-0.7
	Baldy	Pierce	27 07 03.710		16	5.0	-1.8
	Pierce	Rufus	24 51 16.115		17		-1.1
	Gold	Pierce	44 26 45.610		14		2.7
Wanch	Gold	Baldy	42 00 40.710		7	2.6	-1.3
	Baldy	Conuma	37 45 28.210		10	3.9	1.6
	Pierce	Rufus	23 22 39.6 5		18		**
	Pierce	Conuma	35 09 22.310		9		-1.9
	Conuma	Walker	18 15 41.315		12		3.1

---

* Two values indicate the angle was derived from the sum or difference of angles to an intermediate station.

** Angle change not used in strain calculation because only 5 sets were observed or the angle was rejected.

TABLE 2.2 1947 Triangle Closure

STA 1	STA 2	STA 3	EXCESS (s)	CLOSURE (s)	COR. CLOSURE
Wanch	Gold	Baldy H	0.7	7.5	6.8
Wanch	Baldy H	Conuma	0.7	1.1	0.4
Wanch	Gold	Conuma	0.8	7.4	6.6
Conuma	Gold	Baldy H	0.6	-1.9	-2.5
Conuma	Baldy H	Walker	0.6	2.9	2.3
Baldy H	Pierce	Walker	1.2	2.8	1.4
Conuma	Baldy H	Pierce	0.4	-2.8	-3.2
Conuma	Pierce	Walker	1.4	1.5	0.1
Conuma	Baldy H	Rufus	0.9	1.6	0.7
Baldy H	Rufus	Walker	1.4	1.3	-0.1
Conuma	Rufus	Walker	1.1	-3.5	-4.6
Baldy H	Pierce	Rufus	0.7	1.5	0.8
Conuma	Pierce	Rufus	1.1	4.4	3.3
Pierce	Pretty G	Rufus	0.4	2.5	2.1
Gold	Pierce	Baldy H	0.4	4.3	3.9
Gold	Conuma	Pierce	1.5	-0.2	-1.7

The standard deviation of an observed angle may be approximated from the average triangle closure by (Bomford, 1971)

$$\sigma = \sqrt{(\Sigma\ \epsilon^2/3N)}$$

where ϵ is the individual triangle closure corrected for spherical excess and N is the number of closures.

The 16 triangle closures listed in Table 2.2 give the standard deviation for an observed angle of 1.9 s.

The observational error may also be estimated by using the observations in a least-squares adjustment for the station positions. The method used is a weighted variation of coordinate adjustment (Anderson, 1969), which determines the most probable position of the stations. The adjustment program requires input in the form of oriented direction lists. The standard deviation of an observed direction is determined from the difference between the observed directions corrected for orientation and the adjusted directions. For an observation of weight unity the standard deviation is given by

$$\sigma = \sqrt{[\Sigma w(i)v(i)/N-(2NS+NZ)]}$$

where N = total number of observations

w(i) = weight of an observation

v(i) = the residual (observed - adjusted)

NS= the number of new stations

NZ= the number of observation stations used

The expression 2NS + NZ represents the total of independent unknowns.

The adjustment provides the coordinates for each station in the form of latitudes and longitudes. The 1947 observations consist of only angles making it necessary to provide to the adjustment both positional and scale control. This may be done by fixing the position of two stations. Alternatively, a fixed station, a fixed azimuth, and a scale length may be used. This option was chosen, fixing the position of Pierce and the azimuth from Pierce to Gold for position control, and the 1982 length from Pierce to Baldy High for scale control. There is no advantage in this option relative to the two fixed station option.

To convert the angles in Table 2.1 to the oriented direction lists in Table 2.3, the following procedure was used. Angles from an observation station were divided into groups of angles with common adjacent sides. An approximate azimuth was found between the observation station and one of the target stations not common with any other angle in the group. The observed angle between the chosen target station and an adjacent station was added to this initial direction to obtain the direction to the adjacent station. This direction was then used to obtain the directions to the next station within the group. The procedure was repeated for all adjacent angles within a group. The procedure of getting an initial direction and forming a direction list was repeated for the

other groups from the same observing station, and then for other observing stations. Each group of directions will have a common orientation correction, and is identified by its Z number. 23 groups of angles were formed to accommodate the 57 angles observed from the 10 stations. The directions were weighted by the number of sets measured. Those with 10 sets were given a weight of 1.0 and those with 5 a weight of 0.5.

Table 2.3. Oriented 1947 directions

Z No.	Sta 1	Sta 2	Azi ° ' "	Wt.
1	Wanch	Gold	308 19 30.7	
		Baldy	350 20 11.4	
		Rufus		Rej*
		Conuma	028 05 39.6	
2	Wanch	Pierce	352 56 17.3	
		Conuma	028 05 39.6	
		Walker	046 21 20.9	
3	Gold	Pierce	016 28 20.0	0.5
		Baldy	035 20 13.0	
		Conuma	075 44 23.5	
		Wanch	128 28 10.3	
4	New	Pierce	330 25 55.0	0.5
		Conuma	335 09 23.8	0.5
		Rufus	003 20 37.8	0.5
		Walker	050 49 38.8	0.5
5	Conuma	Wanch	208 00 07.0	
		Gold	255 30 18.7	
		Baldy	300 38 13.5	
		Pierce	329 41 28.1	
		Rufus	007 53 36.6	
		Walker	062 52 02.4	
		New	155 10 29.5	0.5
6	Baldy	Pierce	356 58 21.0	
		Rufus	042 02 39.5	
		Walker	087 01 46.6	
		Conuma	120 46 15.0	
		Wanch	170 22 41.5	
		Gold	215 14 10.2	
7	Baldy	Conuma	120 46 15.0	
		Gold	215 14 07.8	
		Pierce	356 58 17.3	
8	Walker	Wanch	226 04 26	0.5
		New	230 39 22	0.5
9	Walker	Wanch	226 04 26.0	
		Conuma	242 40 43.7	
		Baldy	266 42 29.2	
		Pierce	293 49 32.9	
		Rufus	318 40 49.0	
10	Walker	Conuma	242 40 43.7	
		Rufus	318 40 42.9	
11	Walker	Conuma	242 40 43.7	
		Pierce	293 49 28.9	

Table 2.3 Oriented 1947 directions (cont.)

Z No.	Sta 1	Sta 2	Azi ° ' "	Wt.
12	Walker	Gold	249 22 43.3	
		Pierce	293 49 28.9	
13	Rufus	Albermarle	079 34 48.8	0.5
		Walker	138 49 48	0.5
		New	183 19 30.6	0.5
14	Rufus	Walker	138 49 48	
		Conuma	187 51 19.5	
		Wanch	196 11 03.3	
15	Rufus	Pierce	261 54 53.4	
		Pretty	318 34 04.3	
		Albermarle	079 34 58.8	0.5
		Pierce	261 54 54.3	
16	Rufus	Conuma	187 51 19.5	
		Gold	219 09 29.6	
		Pierce	261 54 42.4	
17	Rufus	Conuma	187 51 19.5	
		Baldy	221 52 22.4	
		Pierce	261 54 52.5	
18	Albermarle	Rufus	259 30 05.0	
		Pretty	296 07 47.3	
19	Pretty	Rufus	138 39 01	
		Pierce	219 00 36.6	
20	Pierce	Pretty	039 06 24.8	
		Albermarle	081 22 47.7	
21	Pierce	Pretty	039 06 24.8	
		Rufus	082 05 41.7	
		Walker	114 09 22.3	
		Conuma	149 50 04.3	
		Wanch	172 59 19.7	
		Gold	196 22 50.8	
22	Pierce	Rufus	082 05 41.7	
		Conuma	149 50 06.1	
		Baldy	176 58 54.6	
		Gold	196 22 56.4	Rej*
23	Pierce	New	150 35 35	0.5
		Baldy	176 58 49.0	0.5

---

* These directions were rejected because of large residuals in the adjustment.

The standard deviation of a direction of weight unity from the adjustment for station position is 1.8 s, with a maximum residual of 3.3 s. The standard deviation of an angle is 2.6 s, since it is the difference of two directions. This

is slightly higher than the 1.9 s derived from the triangle closures, but it is obtained from a larger set of observations and, thus, is likely to be a more representative figure.

Survey measurements are often classified by their accuracy, with first-order work being the most accurate and fourth-order work being the least accurate. For second order directions the guidelines from the Survey and Mapping Branch (Div. of Energy, Mines, and Resources, 1973) specify a minimum of 6 sets with the standard deviation of a direction being 2.0 s, and triangle closure less than 5.0 s. The 1947 survey meets all these criteria.

3. STRAIN ACCUMULATION 1946-1982

The change in angles common to the 1947 and 1982 surveys allow computation of the shear components of surface strain accumulation. Scale and absolute azimuth control in the 1947 survey are not adequate to define the dilatational or rotational components of strain. That is, only the angle measurements are accurate enough to extract possible low level strain accumulation. Angles for the 1982 trilateration survey are calculated from the azimuths derived from the adjusted station positions. Thus, any observed or adjusted angle from the 1947 survey can be compared with a corresponding angle from the 1982 survey provided that the stations are common to both surveys. Because most of the angles of interest are between stations tied to the 1982 trilateration by horizontal angles and end-point reduced distances, the error in an angle is greater than that for the primary stations. An error of 0.3s is arbitrarily estimated for an angle derived from the adjusted positions of these stations.

3.1 SHEAR STRAIN FROM ANGLE CHANGES

The shear components of surface strain defined in terms of the tensor components with the 1 axis oriented to the east and the 2 axis north are

$$\gamma_1 = \epsilon_{11} - \epsilon_{22}$$

$$\gamma_2 = 2\epsilon_{12}$$

A positive γ_1 corresponds to pure shear with a north-south axis of compression, and a positive γ_2 corresponds to a pure shear with a northwest-southeast axis of compression. In combination with an equal and opposite rotation a positive γ_1 corresponds to a simple shear with right-lateral motion across a NW-SE line or left-lateral motion across a NE-SW line. Similarly, a positive γ_2 coresponds to a simple shear with right-lateral motion across an E-W line or left-lateral motion across a N-S line. A shear strain field consisting of a combination of the shear components may be represented by the total shear γ and the azimuth of the axis of maximum compression ζ where

$$\gamma = \sqrt{(\gamma_1^2+\gamma_2^2)}$$

$$\zeta = 1/2\arctan(-\gamma_2/\gamma_1) \text{ if } \gamma_2/\gamma_1<0$$

$$\zeta = \zeta + \pi/4 \text{ if } \gamma_2/\gamma_1>0$$

An alternative representation uses the magnitude and directions of the principal deviatoric strains related to γ by

$$\gamma = \epsilon 1-\epsilon 2$$

where $\epsilon 1$ is the maximum extensional strain and $\epsilon 2$ is the maximum compressional strain. The orientation is given by ζ. The deviatoric principle strains are constrained to be equal in magnitude but opposite in sign.

The change in an angle is related to the shear components of strain (Frank, 1967) by

$$\delta\phi = 1/2(\sin 2\theta_2 - \sin 2\theta_1)\gamma_1 + 1/2(\cos 2\theta_2 - \cos 2\theta_1)\gamma_2$$

where θ_1 and θ_2 are the oriented directions enclosing the angle ϕ. The orientation need only be approximate.

Given two or more suitably oriented angles γ_1 and γ_2 are theoretically determined. However, observational error may account for some or all of the angle change. For a small number of repeated angles the standard deviation in the total shear may be approximated by the standard deviation of the difference of an observed angle. Using 2.6 s for the standard deviation an angle measurement in the 1947 survey and 0.3 s for the 1982 survey, the standard deviation for an angle change is 2.7 s, or 12 μrad. If we assume tectonic strain of 0.2 μrad per year, a value typical in active areas (Savage, 1983), it would take 60 years of average tectonic strain to exceed the observational error of an angle.

The detection threshold, or noise level for strain accumulation may be reduced by using a large number of angle changes in a least-squares solution for the most probable values of the shear strain components. This method assumes uniform strain across the portion of the network included in the calculation. Details of the method, generalized for any collection of angles and an arbitrary number of surveys, are given by Prescott (1976). Prescott's method includes the additional assumption that strain accumulates at a constant rate, and results are stated in terms of strain rates. Shear strain accumulation in the Gold River network is given in

terms of strain rates to allow comparison with other measurements that cover different areas and time periods. The standard deviation of the shear strain from a set of N repeated angle observations should be about $\sigma\sqrt{(8/N)}$, where σ is the standard deviation of an angle change (Savage, 1983). For the Gold River network this is 5 μrad or, dividing it by the 35 years between the surveys, 0.14 μrad per year.

3.2 CALCULATED SHEAR STRAIN 1947-1982

Observed and adjusted angles from the 1947 survey are compared with angles calculated from the adjusted station positions from the 1982 survey to determine the shear strain accumulation. The difference between the 1982 and 1947 observed value of an angle is shown in Table 2.1. The input for the shear strain calculation is the same list of directions used for the 1947 adjustment (Table 2.3) plus a corresponding list of directions calculated from the 1982 adjustment. To obtain a uniform data set, only 1947 angles with 10 or more turns were used to form the direction lists.

The shear strain calculation was performed for the entire network and for two subsets labelled north and south. The northern subset includes all angles between the stations Baldy High, Conuma, Wanch, and Gold while the southern subset includes all angles between the stations Baldy High, Conuma, Walker, Rufus, Pierce, Pretty Girl, and Albermarle. It should be noted that the two subsets contain a different number of angles and that the set of observations used for the entire

network includes angles that are not in either subset. The rate of shear strain accumulation is listed in Table 3.1. The standard deviations are derived from the least squares fit to a uniform strain field. The theoretical standard deviation for the shear strain may be obtained by dividing the experimental values listed in Table 3.1 by r, the ratio of observed to theoretical error.

TABLE 3.1 Shear strain accumulation

AREA	γ_1 μrad	γ_2 μrad	γ μrad	ζ °from N	r
NETWORK	0.03 ±0.12	0.03 ±0.14	0.03 ±0.13	*	1.3
NORTH	0.38 ±0.21	-0.40 ±0.30	0.54 ±0.31	23 ±10	1.1
SOUTH	-0.19 ±0.14	-0.05 ±0.15	0.20 ±0.14	82 ±22	1.2
ADJUSTED ANGLES					
NETWORK	-0.01 ±0.06	-0.03 ±0.07	0.03 ±0.07	*	0.6
NORTH	0.16 ±0.23	-0.17 ±0.30	0.23 ±0.30	23 ±26	1.0
SOUTH	-0.22 ±0.06	-0.14 ±0.07	0.25 ±0.07	74 ±07	0.5

* Direction is uncertain.

As seen in Table 3.1 there is no significant strain accumulation at the two standard deviation level in the network or in the subsets of the network. The value of r is near 1 indicating that the angle change, or lack of change in this case, is uniform across the network and within the error estimated for an angle change. Both the north and south subsets show strain accumulation at the one standard deviation

level.

A similar set of strain calculations were performed substituting angles calculated from the 1947 adjustment for the observed angles. The 1947 adjustment provides the most probable positions for the stations and, therfore, the most probable value for the angles. The direction lists are simplified from those used for the observed angles by having only one direction list from each observing station. Caution is advised when using adjusted angles supplied by another agency. Often the angles are derived from a mix of surveys made during different periods or they may be contaminated by data to stations outside of the area of interest.

The results from the comparison of the adjusted angles from both surveys, also shown in Table 3.1, are similar to those from the observed angles, except the ratio of observed to theoretical error is decreased. This is expected as the error in an adjusted direction is less than that for an observed direction. There is no significant strain accumulation at the one standard deviation level in the entire network or in the north subset. Only the south subset shows significant strain accumulation at the two standard deviation level.

These results are different than those given in the preliminary reports for the study. The rates of strain accumulation reported in May of 1983 at the G.A.S.C. meeting in Victoria were derived from a set of angles used as input for a B.C. Ministry of Survey's adjustment for central

Vancouver Island. The angles were not a complete set and contained some adjusted angles, possibly from a local adjustment. The next set of results were reported at the Pacific Northwest A.G.U. meeting in Bellingham in October 1984. These results are from the correct set of angles observations, but the direction lists were formed different manner which is belived to be incorrect.

REFERENCES

Anderson, W.L., Weighted triangulation adjustment, U.S. Geol. Sur. Open-file report Computer Contribution number 1, U.S. Geological Survey Computer Center Division, Washington D.C., 52 pp, 1969.

Berg, E., D. Harris, and C.A. Fisher, High precision single color laser distances, techniques and procedures to approach 0.3 ppM. Maui, Lanai, and Molokai network, Hawaii Institute of Geophysics, 209 pp, 1981.

Bomford, G., Geodesy, 3rd edition, pp , Oxford Press, London, 1971.

Dept. of Energy, Mines, and Resources, Specifications and recommendations for control surveys and survey markers, Survey and Mapping Branch misc. ser. 73/3, p 17, 1973.

Frank, F.C., Deduction of earth strains from survey data, Bull. Seismol. Soc. Am., 51, 35-42, 1967.

Greene, J.R., Accuracy evaluation in electro-optic distance measuring instruments, Surveying and Mapping, 37, 247-256, 1977.

Hilton, W.F., Thermal effects on bodies in an airstream, Proc. Roy. Soc. London, Ser. A, 168, 43-56,1938.

Omega Engineering, 1984 Complete Temperature Handbook and Encyclopedia , Omega Engineering Inc., Samford Ct., 1984.

Owens, J.C. Optical refractive index of air: dependence on pressure, temperature and composition, Appl. Opt., 6, 51-59, 1967.

Prescott, W.H., An extension of Frank's method for obtaining

crustal shear strains from survey data, Bull. Seismol. Soc. Am., 66, 1847-1853, 1976.

Rinner, K., Distance measurement with the aid of electromagnetic waves, Geophys. Surveys, 1, 459-479, 1974.

Savage, J.C., Strain accumulation in western United States, Ann. Rev. Earth Planet. Sci., 11, 11-43, 1983

Savage J.C. and W.H. Prescott, Precision of geodolite distance measurements foe determining fault movements, J. Geophys. Res., 78, 6001-6008, 1973.

Stickney, T.M., M.W. Shedlov, D.I. Thompson, F.T. Yakos, Rosemount total temperature sensors, Technical Report 5755 Revision A, Rosemount Inc, Minnesota, 1981.

Thatcher, W., Crustal deformation studies and earthquake prediction, Eathquake Prediction - an International Review, Maurice Ewing Series, A.G.U., 394-410, 1981.

Trenkle F. and M. Reinhart, In-flight temperature measurements, in Volume 2 of AGARD Flight Test Instrument Series, AGARD-AG-160-Vol 2, 1973.